分 类 号_____ 学号_____D201277241_____

学校代码__10487__ 密级_____

華中科技大學

博 士 学 位 论 文

太阳能光热梯级发电系统设计及其特性研究

学位申请人：张成

学 科 专 业：热能工程

指 导 教 师：高伟 教授

Inmaculada Arauzo 教授

张燕平 副教授

答 辩 日 期：2017 年 9 月 1 日

A Thesis Submitted in Partial Fulfillment of the
Requirements for the Ph.D

Cascade solar thermal power system design and research of the key features

Student : Cheng Zhang

Major : Thermal Engineering

Supervisor : Prof. Wei Gao

Prof. Inmaculada Arauzo

Associate Prof. Yanping Zhang

Huazhong University of Science & Technology

Wuhan 430074, P. R. China

September 1, 2017

独创性声明

本人声明所呈交的学位论文是我个人在导师的指导下进行的研究工作及取得的研究成果。尽我所知，除文中已标明引用的内容外，本论文不包含任何其他人或集体已经发表或撰写过的研究成果。对本文的研究做出贡献的个人和集体，均已在文中以明确方式标明。本人完全意识到本声明的法律结果由本人承担。

学位论文作者签名：

日期：　　年　　月　　日

学位论文版权使用授权书

本学位论文作者完全了解学校有关保留、使用学位论文的规定，即：学校有权保留并向国家有关部门或机构送交论文的复印件和电子版，允许论文被查阅和借阅。本人授权华中科技大学可以将本学位论文的全部或部分内容编入有关数据库进行检索，可以采用影印、缩印或扫描等复制手段保存和汇编本学位论文。

本论文属于　保密 □，在 ____ 年解密后适用本授权书。

　　不保密 □。

（请在以上方框内打“√”）

学位论文作者签名：　　指导教师签名：

日期：　　年　　月　　日　　日期：　　年　　月　　日

摘 要

随着化石能源的消耗和环境问题的凸显，太阳能作为一种新能源，具有分布广泛、总量巨大、取之不竭、无污染的特点，越来越受到世界各国的重视，被广泛认为是未来最有潜力替代传统化石能源的清洁能源。在发电领域，太阳能光热发电是除了太阳能光伏发电之外的另一种发电形式。与光伏发电相比，光热发电因具有发电平稳，电网兼容性友好，易于与现有化石燃料电厂组合等优点而受到越来越多的关注。已经商业应用的太阳能光热发电技术分为槽式集热发电、碟式集热发电和塔式集热发电三种。三种发电技术各有优缺点：槽式集热发电应用最广，成本较低，但效率也较低；碟式集热发电规模较小，多用于分布式发电；塔式集热发电规模较大，成本较高，目前处于快速发展阶段。综合利用现有发电技术的优缺点，在能量梯级收集和能量梯级利用的思想上，提出采用多种集热发电方式和多种热功循环的梯级系统，是实现大规模太阳能光热发电的一种新颖的可行的技术方案。

本课题以国家国际合作项目专项“太阳能梯级集热发电系统关键技术合作研究”为背景，目标是研究太阳能光热发电装置，利用各种传统型式的太阳能光热发电系统的优缺点以及热力特性，提出并组建、优化太阳能梯级集热发电系统，为探索出可大规模高效率利用太阳能的光热发电技术提供新的方案。主要研究内容和结论包括：

首先，提出太阳能光热梯级集热发电系统的拓扑结构。通过热力特性分析，结合系统中各部件的工作特点，合理布局太阳能光热梯级集热发电系统，利用不同热功循环实现不同品位的能量的梯级利用。合理的梯级发电系统方案才能充分利用发电系统中各部件的性能特点，为创建高效率的太阳能光热梯级发电系统提供基础。本文针对系统中的各组件，组建了多种可行的梯级集热系统拓扑结构。经过系统评估、参数选取、初步计算、方案比较，确定了两种具有代表性的太阳能光热梯级发电系统方案。一种方案同时选用水工质朗肯循环和斯特林循环，利用给水来冷却斯特林机冷腔，回收利用斯特林机放出的热量；另一种方案选用多级有机工质朗肯循环，利用上一级的凝集热来加热下一级的循环工质，实现能量的梯级利用。

其次，针对太阳能光热梯级集热发电系统的各部件建立机理模型。依据目标对象的运行机理，根据物理平衡方程，对系统中的各部件，尤其是系统中的关键部件，如集热器、蒸汽产生系统、汽轮机、斯特林机等，建立起数学模型。各部件的数学模型是经由经典理论或是大量实验数据验证的模型，是组建光热梯级集热发电系统模型的基础。对于槽式集热器的集热管和碟式集热器的集热器，建立了热损失模型；对于斯特林机，基于合理的简化和假设，推导出了考虑了各种热损失和不可逆因素的斯特林机

模型。各部件模型使用 MATLAB 语言编写，采用面向对象的方法，充分利用了继承、多态等特性，保证了各部件之间既具有独立性又具有关联性。

再次，组建太阳能光热梯级集热发电系统模型。根据所选择的太阳能光热梯级发电系统方案，基于建立好的系统中各部件的模型，利用面向对象语言的继承、组合、多态等特点，组建起梯级集热发电系统模型。研究系统在外部及内部因素的耦合作用下主要参数及性能指标的变化规律，掌握其变化机理，建立其性能特性的计算方法。经过组建部件，设置参数，编译环境，完成了各系统方案的系统组建工作，最终完成了拥有自主计算机软件著作权的基于 MATLAB 的太阳能光热梯级发电的模拟系统。系统中各部件相对独立，便于更换或改进部件模型；各系统模型的计算结果可以以单个对象的方式方便地查看系统中各个部件的关键参数。

然后，模拟并优化太阳能光热梯级集热发电系统模型。在太阳能光热梯级发电系统性能特性研究的基础上，对系统进行流程优化、结构重构。具体地，通过对系统的蒸汽发生系统进行分析，提出了分阶段加热方法，通过改变导热油的质量流量降低蒸汽发生系统中的传热温差，有效降低了蒸汽发生系统中换热过程中产生的㶲损，进而可以提高整个系统的效率。针对梯级系统中的斯特林机组，总结了斯特林机组所具有的五种基本排列形式，并分析了各种排列形式下机组的效率和输出功率的差异，得到了给定冷热源流体条件下斯特林机组最佳的排列方式。

最后，优化太阳能光热梯级集热发电系统的运行参数。针对特定结构方案和运行模式，以梯级发电系统的性能参数和经济指标为目标函数，选择合理的可调节参数，确立各种约束条件，利用现代优化方法，如基因算法、蚁群算法，完成系统的参数优化分析，以及对于独立系统的对比分析。分析结果表明，太阳能光热梯级集热发电系统在一定的参数条件下，相比其对应的独立系统，具有更高的总体光电转换效率。在太阳直射强度为 700 W/m^2，碟式集热器出口空气温度为 800°C 的条件下，方案 1 所选用的太阳能光热梯级集热发电系统比对应的独立系统效率提升 5.2%，方案 2 所选用的太阳能光热梯级集热发电系统比对应的独立系统效率提升 15.3%。

关键词： 槽式集热器，碟式集热器，朗肯循环，斯特林循环，斯特林机组，梯级发电

Abstract

With the increasing awareness of problem of fossil energy consumption and environmental pollution, solar energy as a renewable energy, which has the advantages of widely distribution, huge amount, inexhaustible and no pollution, has received much attention by many countries and been regarded as the best potential candidate of the fossil energy. Concentrating solar thermal power generation is another form of power generation technology except solar photovoltaic power generation. Compared to solar photovoltaic, solar thermal power is gaining more attention for its advantages as smooth power generation, good grid compatibility, easy to integrate with existing fossil power plant.

Commercial solar thermal power generation technology is divided into trough collector power generation, dish collector power generation and solar tower power generation. These three types of power generation technologies have their own advantages and disadvantages: trough collector power generation is the most widely used one, its cost is low, however its efficiency is also low; dish collector power generation has high efficiency and smaller capacity, it is used for distributed generation widely; solar tower generation, which has large scales, high efficiency and high cost, is currently in rapid development stage. Based on the idea of energy cascade collection and energy cascade utilization, this paper proposed a cascade system that uses different collector power generation methods and different thermodynamic cycles, which may be a new and feasible technology to realize large-scale solar thermal power generation.

The research is based on the national cooperation project ”Collaborative research on key technologies to produce electricity by cascade utilization solar thermal energy” as the background. The objective of this project is to research the equipment of solar thermal power generation system, to propose, develop and optimize a solar thermal cascade system depending on the advantages and disadvantages of the solar thermal power generation system, and to explore a new feasible technology for large-scale solar thermal power generation. The main contents and conclusions of this paper are as follows:

Firstly, the topological structure of solar thermal cascade power generation system was proposed. According to the analysis of thermal characteristics and the working characteristics of each component in the system, rationally arranged topological structures of cascade system were proposed. These systems use different thermodynamic cycles to utilize energy

in different temperature zones. A reasonable cascade generation system can make full use the performance characteristics of the components in the power generation system and provide the foundation for higher efficiency solar thermal cascade generation systems. In this paper, several schemes of feasible topological structures of solar thermal cascade system were set up according to the components in the system. After system evaluation, parameter selection, preliminary calculation and scheme comparison, two representative typical schemes were determined. In one scheme, both Rankine cycle (water as the working fluid) and Stirling cycle are used for power generation. Cooling water of the Rankine cycle is used to cool the hot end of the Stirling engines to recover the released heat. In the other scheme, multiple organic Rankine cycles are used for power generation. Condensation heat of upper cycle is absorbed by lower cycle for energy cascade utilization.

Secondly, mechanism models were established for the components of solar thermal power generation system. The mechanism mathematical models were developed according to the operation mechanism of the target object and physical equations. The key components in the system, such as collectors, steam generating system, steam turbine and Stirling engine, were modeled with details. The mathematical model of each component is a model verified by the classical theory or a large number of experimental data, which is the basic of the model of the cascade solar thermal power generation system. Heat loss models were established for the receivers of trough collector and dish collector. For the Stirling engine, based on the reasonable simplification and hypothesis, the model of the Stirling machine considered various losses and irrevisibilities was developed. The component models were developed in MATLAB by using object-oriented method. It makes full use of inheritance and polymorphism to ensure both the independence and the relevance of the components.

Thirdly, the solar thermal cascade generation system models were developed. Based on the selected solar thermal cascade generation systems, solar thermal cascade generation system models were established based on the model of each component in the systems. The object-oriented features of inheritance, combination and polymorphism were used for the model development. The change rules of the main parameters and the performance indexes under the coupling of external and internal factors were studied. The change mechanism was studied and the calculation method of its performance characteristics was established. After setting up the components, setting the parameters and compiling the environment, the paper completes the system construction of each system scheme, and finally completes the simulation system of solar thermal cascade generation based on MATLAB with the copyright of independent computer software. The system components are relatively independent, easy

to replace or improve the parts model; the results of the calculation of the system model can be a single object to easily view the various components of the system key parameters.

Then, simulation and optimization of cascade solar thermal power generation system model. Based on the study of the performance characteristics of solar thermal cascade generation system, the system is optimized and the structure is reconstructed. In particular, by analyzing the steam generation system of the system, a method of staged heating is proposed to reduce the heat transfer temperature difference in the steam generating system by changing the mass flow rate of the heat conduction oil, effectively reducing the heat generated during the heat exchange process in the steam generating system. Which can improve the efficiency of the whole system. Based on Stirling unit in cascade system, five kinds of basic arrangement forms of Stirling unit are summarized, and the difference of unit efficiency and output power under various arrangement forms is analyzed, and a given cold and heat source fluid Stirling unit under the conditions of the best arrangement.

Finally, the operating parameters of solar thermal cascade power generation system are optimized. According to the specific structural scheme and operation mode, the performance parameters and economic indexes of the cascade generation system are taken as the objective function, reasonable adjustable parameters are selected, various constraints are established, and modern optimization methods such as genetic algorithm and ant colony algorithm are used to complete the system Parameter optimization analysis, as well as the independent system for comparative analysis. The results show that solar thermal cascade power generation system has higher overall photoelectric conversion efficiency under certain parameter conditions than its corresponding independent system. Under the condition of direct solar radiation intensity of $700\,\mathrm{W/m^2}$ and dish type collector outlet air temperature of 800°C, the solar thermal cascade power generation system of Scheme 1 is better than the corresponding The efficiency of stand-alone system is increased by 5.2%. The solar thermal cascade power generation system selected in Scheme 2 is 15.3% more efficient than the corresponding independent system.

Key words: parabolic trough collector, parabolic dish collector, Rankine cycle, Stirling cycle, Stirling engine array, cascade powering

Contents

Nomenclature

$\dot{m}$ Mass flow rate, kg/s

A heat transfer area (m^2)

$A_{dr,1}$ Heat transfer area of dish receiver between tube and air, m^2

$A_{se,1}$ Heat transfer area of Stirling engine at air side, m^2

$A_{se,2}$ Heat transfer area of Stirling engine at water side, m^2

c_p specific heat at constant pressure ($J{\cdot}kg^{-1}{\cdot}K^{-1}$)

c_r Heat transfer correction factor of coiled tube of volumetric receiver

c_v specific heat at constant volume ($J{\cdot}kg^{-1}{\cdot}K^{-1}$)

d Diameter, m

dep Depth, m

J annular gap cylinder displacer (m)

K dead volume factor

k Specific heat ratio

k specific heat ratio (c_p/c_v), thermal conductivity ($W \cdot m^{-1} \cdot K^{-1}$)

k_{insu} Thermal conductivity of air at the temperature of outside insulating layer, W/(m·K)

m mass of working fluid in Stirling engine (kg)

n Number of collectors

n_1 Number of columns of the Stirling engine array,

Number of rows of the Stirling engine array

Amount of working gas in each Stirling engine, mol

Number of Stirling engines in the Stirling engine array

number of Stirling engine in SEA

Nusselt number

power of Stirling engine (W)

pressure (Pa)

Extraction pressure of the steam turbine, MPa

Prandtl number

absorbed heat (J)

Heat flux

mass flow rate ($kg \cdot s^{-1}$)

gas constant ($J \cdot kg^{-1} \cdot K^{-1}$)

Reynolds number

speed of Stirling engine (Hz)

wall temperature (K)

overall heat transfer coefficient ($W \cdot m^{-2} \cdot K^{-1}$)

compression volume (m^3)

total dead volume (m^3)

expansion volume (m^3)

cold space dead volume (m^3)

hot space dead volume (m^3)

regenerator dead volume (m^3)

output work (J)

Dryness fraction

Extraction rate of steam turbine

displacer stroke (m)

List of Figures

List of Tables

footnotefootnote # Chapter 1

Introduction

Saving our planet, lifting people out of poverty, advancing economic growth... these are one and the same fight. We must connect the dots between climate change, water scarcity, energy shortages, global health, food security and women's empowerment. Solutions to one problem must be solutions for all.*Ban Ki-moon*

This dissertation considers a way to solve the global problems of energy shortage and environment problem.

1.1 Research background and significance

REN21, a global renewable energy policy multi-stakeholder network, published the most comprehensive annual overview of renewable energy of 2016. [**?**] Renewables are now established around the world as mainstream sources of energy. Rapid growth, particularly in the power sector, is driven by several factors, including the improving cost-competiveness of renewable technologies, dedicated policy initiatives, better access to financing, energy security and environmental concerns, growing demand for energy in developing and emerging economies, and the need for access to modern energy.

Solar energy, which has the advantages of widely distribution, huge amount, inexhaustible and no pollution, has received much attention by many countries and been regarded as the best potential candidate of the fossil energy. The International Energy Agency projected in 2014 that under its "high renewables" scenario, by

2050, solar photovoltaics and concentrating solar power would contribute about 16 and 11 percent, respectively, of the worldwide electricity consumption, and solar would be the world's largest source of electricity. [**?**]

Concentrating solar thermal power generation is another form of power generation technology except solar photovoltaic power generation. Concentrating Solar Power (CSP) energy system uses mirrors to converge sunlight onto a receiver that absorbs the solar energy and transfer it to a heat transfer fluid (HTF) such as a synthetic oil, molten salt or air. The HTF then directly or indirectly used as the heat source in a power cycle. Compared to solar photovoltaic, solar thermal power is gaining more attention for its advantages as higher energy density, smooth power generation, good grid compatibility, easy to integrate with existing fossil power plant.

Concentrating solar power technologies use different mirror configurations to concentrate the sun's light energy onto a receiver and convert it into heat. The heat can then be used to create steam to drive a turbine to produce electrical power or used as industrial process heat. There are three types of CSP technologies being commercialy applied: parabolic trough, parabolic dish and power tower.

A parabolic trough is a type of solar thermal collector whose mirror type is straight in one dimension and curved as a parabola in the other two. The reflector follows the sun during the daylight hours by tracking along a single axis. The energy of sunlight is reflected by the mirror and focused on the pipe positioned at the focal line. HTF (e.g. synthetic oil) runs through the pipe to absorb the heat generated by the focused sunlight, then used as the heat source for heating process or power generation. Figure

A parabolic dish is a type of solar thermal collector whose mirror type is part of a circular paraboloid, that can converging the incoming sunlight traveling along the axis to the focus. A receiver or Stirling engine is put at the focal point to absorb the converged energy. Figure

A solar power tower is a type of solar furnace using a tower to receive the focused sunlight. It uses an array of flat, movable mirrors (called heliostats) to focus the sun's rays upon a collector tower (the target). Figure

Among the three solar thermal power technologies, parabolic trough is the

Figure 1.1: Alpha-Trough-350, a parabolic trough product made by Alpha-E

most mature and commercially deployed technology. However, it has a low concentration ratio, the receiver's temperature is relatively low, the solar-to-electric efficiency is relatively low. Parabolic dish can obtain high temperature thermal energy, it's solar-to-electric can be higher than parabolic trough. Besides, one advantage of parabolic trough is that it requires much less water for power generation. However, solar parabolic dish is not a large-scale application, it's mainly applied for distributed power generation for its compact structure and easy installation. Solar power tower has a very high concentration ratio when more mirrors (also called heliostats) are used, the receiver's temperature can be very high and it can be applied for large-scale application. However, it has some disadvantages such as high investment. It is currently in rapid development stage.

It is very important to find out a way the utilize the advantages of existing solar thermal power technologies and overcome their disadvantages. In other words, to find out a new technology with higher efficiency lower cost is urgent. This research is trying to achieve this by proposing a cascade system that uses different collector power generation methods and different thermodynamic cycles, which may be a new and feasible technology to realize large-scale solar thermal power generation.

Figure 1.2: A 38 kW prototype Stirling engine product of XEMC

1.2 State of the art

1.2.1 Parabolic trough

Parabolic trough solar technology is the most proven and lowest cost large-scale solar power technology available. [**?**]

Padilla [**?**] performed a detailed one dimensional numerical heat transfer analysis of a PTC (Parabolic Trough Collector). To solve the mathematical model of

Figure 1.3: Overall view of Solar Two power tower

heat transfer of the PTC model, the partial differential equations were discretized and the nonlinear algebraic equations were solved simultaneously. The numerical results was validated to the data from Sandia National Laboratory (SNL). [C]PTCParabolic Trough Collector [C]SNLSandia National Laboratory

To understand the thermal performance of the collector and identify the heat losses from the collector, Mohamad [**?**] analyzed the temperature variation of the working fluid, tube and glass along the collector.

Guo [**?**] investigated the energy efficiency and exergy efficiency of the parabolic trough collector. The result shown that there exists an optimal mass flow rate of working fluid for exergy efficiency, and the thermal efficiency and exergy efficiency have opposite changing tendencies under some conditions.

Guo [**?**] implemented a multi-parameter optimization of parabolic trough solar receiver based on genetic algorithm where Exergy and thermal efficiencies were employed as objective function.

Padilla [**?**] performed a comprehensive exergy balance of a parabolic trough collector based on the previous heat transfer model [**?**]. The results shown that inlet temperature of heat transfer fluid, solar irradiance, and vacuum in annulus have a significant effect on the thermal and exergetic performance, but the effect of wind speed and mass flow rate of heat transfer fluid is negligible. It was obtained that inlet temperature of heat transfer fluid cannot be optimized to achieve simultaneously maximum thermal and exergetic efficiency because they exhibit opposite trends. Finally, it was found that the highest exergy destruction is due to the heat transfer between the sun and the absorber while for exergy losses is due to optical error.

Huang [**?**] proposed an analytical model for optical performance which employed a modified integration algorithm.

Wang [**?**] proposed a mathematical model for the optical efficiency of the parabolic trough solar collector and selected three typical regions of solar thermal utilization in China for the model. The model is validated by comparing the test results in parabolic trough power plant, with relative error range of 1% to about 5%.

Al-Sulaiman [**?**] presented the exergy analysis of selected thermal power systems driven by PTSCs. The power pf the thermal power system is produced using either a steam Rankine cycle (SRC) or a combined cycle, in which the SRC is the topping cycle and an organic Rankine cycle (ORC) is the bottoming cycle. [C]SRCSteam Rankine Cycle [C]ORCOrganic Rankine Cycle

Hachicha [**?**] presented a detailed numerical heat transfer model based on the finite volume method for the parabolic trough collector. This model is based on finite volume method and ray trace techniques and takes into account the finite size of the Sun. The model is thoroughly validated with results from the literature and it shows a good agreement with experimental and analytical results.

Ashouri [**?**] coupled a small scale parabolic trough collector and a thermal storage tank along with an auxiliary heater to a Kalina cycle to study the performance of the system throughout the year, both thermodynamically and economically.

Guo [**?**] developed a nonlinear distribution parameter model to model the dynamic behaviors of direct steam generation parabolic trough collector loops under either full or partial solar irradiance disturbance.

Bader [**?**] developed a numerical model of a tubular vavity-receiver that uses air as the heat transfer fluid. Four different receiver configurations are considered, with smooth or V-corrugated absorber tube and single- or double-glazed aperture window. The different types of energy loss by the collector have been quantified, and the temperature distribution inside the receiver has been studied. The pumping power required to pump the HTF through the receiver has been determined for a 200 m long collector row.

Good [**?**] proposed solar trough concentrators using air as heat transfer fluid at operating temperatures exceeding $600\,^{\circ}$C. It consists of an array of helically coiled absorber tubes contained side-by-side within an insulated groove having a rectangular windowed opening. Secondary concentrating optics are incorporated to boost the geometric concentration ratio to $97\times$.

Boukelia [**?**] investigated the feed-forward back-propagation learning algorithm with three different variants; Levenberge Marguardt (LM), Scaled Conjugate Gradient (SCG), and Pola-Ribiere Conjugate Gradient (PCG), used in artificial neural network (ANN) to find the best approach for prediction and techno-economic optimization of parabolic trough solar thermal power plant (PTSTPP) integrated with fuel backup system and thermal energy storage. [C]LMLevenberge Marguardt [C]SCGScaled Conjugate Gradient [C]PCGPola-Ribiere Conjugate Gradient [C]ANNArtificial Neural Network [C]PTSTPPParabolic Trough Solar Thermal Power Plant

Kaloudis [**?**] investigated a PTC system with nanofluid as the HTF in terms of Computational Fluid Dynamics (CFD). Syltherm 800 liquid oil was used as the HTF, and Al_2O_3 nanoparticles with the concentrations ranges from 0% to 4% was investigated. A boost up to 10% on the collector efficiency was reported for Al_2O_3 concentration of 4%. [C]HTFHeat Transfer Fluid [C]CFDComputational Fluid Dynamics

Tan [**?**] proposed a two-stage photovoltaic thermal system based on solar trough concentration is proposed, in which the metal cavity heating stage is added

on the basis of the PV/T stage, and thermal energy with higher temperature is output while electric energy is output. The experimental platform of the two-stage photovoltaic thermal system was established, with a 1.8 m^2 mirror PV/T stage and a 15 m^2 mirror heating stage, or a 1.8 m^2 mirror PV/T stage and a 30 m^2 mirror heating stage. The results showed that with single cycle, the long metal cavity heating stage would bring lower thermal efficiency, but temperature rise of the working medium is higher, up to 12.06 ∘C with only single cycle. With 30 min closed multiple cycles, the temperature of the working medium in the water tank was 62.8 ∘C, with an increase of 28.7 ∘C, and thermal energy with higher temperature could be output.

Al-Sulaiman [**?**] proposed a novel system based on PTC and ORC for combined cooling, heating and power (CCHP). Performance assessment, including efficiency, net electrical power, and electrical to heating and cooling ratios, of the system shown that when CCHP is used, the efficiency increases significantly. This study reveals that the maximum electrical efficiency for the solar mode is 15%, for the solar and storage mode is 7%, and for the storage mode is 6.5%. The maximum CCHP efficiency for the solar mode is 94%, for the solar and storage mode is 47%, and for the storage mode is 42%. [C]CCHPCombined cooling, heating and power

Lobon [**?**] introduced a computational fluid dynamic simulation approach to predict the behavior of a solar steam generating system, which is located at the Plataforma Solar de Almeria, Spain. The CFD package STAR-CCM+ code has been used to implement an efficient multiphase model capable of simulating the dynamics of the multiphase fluid in parabolic-trough solar collectors. Numerical and experimental data are compared in a wide range of working conditions. [C]DSGDirect Steam Generation

Xu [**?**] presented a method to compensate the end loss effect of PTC. An optical analysis on the end loss effect of PTC with horizontal north-south axis (PTC-HNSA) is performed and a five-meter PTC-HNSA experimental system was built. The increased thermal efficiency of the experimental system is measured, and the result that the experimental value (increased thermal efficiency) substantially agreed with the theoretical value (increased optical efficiency) is gained.

Liu [**?**] developed a mathematical model of PTC using the least squares support vector machine (LSSVM) method. Numerical simulations are implemented to evaluate the feasibility and efficiency of the LSSVM method, where the sample data derived from the experiment and the simulation results of two solar collector systems with 30 m^2 and 600 m^2 solar fields, and the complicated relationship between the solar collector efficiency and the solar flux, the flow rate and the inlet temperature of the heat transfer fluid (HTF) is extracted. [C]LSSVMLeast squares support vector machine

1.2.2 Parabolic dish

One of the main goals of the BIOSTIRLING-4SKA project, funded by the European Commission, is the development of a hybrid Dish-Stirling system based on a hybrid solar-gas receiver, which has been designed by the Swedish company Cleanergy [**?**].

Craig [**?**] proposed two types of cooking sections of the solar parabolic dish system: the spiral hot plate copper tube and the heat pipe plate. A conical cavity of copper tubes were put on the focus of the collectors to collect heat and the heat is stored inside an insulated tank which acts both as storage and cooking plate. The use of heat pipes to transfer heat between the oil storage and the cooking pot was compared to the use of a direct natural syphon principle which is achieved using copper tubes in spiral form like electric stove. An accurate theoretical analysis for the heat pipe cooker was achieved by solving the boiling and vaporization in the evaporator side and then balancing it with the condensation and liquid-vapor interaction in the condenser part while correct heat transfer, pressure and height balancing was calculated in the second experiment. The results show and compare the cooking time, boiling characteristics, overall utilization efficiencies and necessary comparison between the two system and other existing systems.

Flux distribution of the receiver is simulated successfully by Mao [**?**] using MCRT method. The impacts of incident solar irradiation, aspect ratio (the ratio of the receiver height to the receiver diameter), and system error on the radiation flux of the receiver are investigated. [C]MCRTMonte Carlo Ray Tracing

Mawire [?] investigated the thermal performance of a cylindrical cavity receiver for an SK-14 parabolic dish concentrator. The receiver exergy rates and efficiencies are found to be appreciably smaller than the receiver energy rates and efficiencies. The exergy factor is found to be high under conditions of high solar radiation and under high operating temperatures. An optical efficiency of around 52% for parabolic dish system is determined under high solar radiation conditions.

Reddy [?, ?] performed the theoretical thermal performance analysis of a fuzzy focal solar parabolic dish concentrator with modified cavity receiver. Total heat loss from the modified cavity receiver is estimated considering the effects of wind conditions, operating temperature, emissivity of the cavity cover and thickness of insulation. Time constant test was carried out to determine the influence of sudden change in solar radiation at steady state conditions. The daily performance tests were conducted for different flow rates.

Vikram [?] investigated the total heat losses of modified cavity receiver of SPD with three configurations using 3D numerical model. The effects of various parameters such as diameter ratio, angle of inclination, operating temperature, insulation thickness and emissivity of the cavity cover on the heat losses from the modified vavity receiver are investigated. An ANN model is developed to predict the heat loss for a large set of influencing parameters. Based on ANN modeling, improved Nusselt number correlations are proposed for convective, radiative and total heat losses from the modified cavity receiver. The convective heat losses are greatly influenced by receiver inclination whereas the radiation heat losses are influenced by the cavity cover emissivity. The diameter ratio also plays a major role in heat losses from the cavity receiver. The present method predicts the heat losses more accurately compared with the existing models.

Atul [?] proposed a low-cost solar dish water heating system and investigated the effect of variation of mass flow rate on performance of the heater prototype. A novel truncated cone-shaped helical coiled receiver made up of copper is put at the focal point of SP.

CRTEn developed a solar parabolic concentrator (SPC) using four types of absorbers: flat plat, disk, water calorimeter and solar heat exchanger. [?] For the system different types of absorbers, experiments were conducted to obtain the mean

concentration ratio and both energy and exergy efficiency. Results shown that thermal energy efficiency of the system varies from 40% to 77%, the concentrating system reaches an average exergy efficiency of 50% and a concentration factor around 178. [C]CRTEnResearch and Technologies Centre of Energy in Borj Cedria [C]SPCSolar parabolic concentrator

Blazquez [**?**] studied the optimization of the concentrator and receiver cavity geometry of parabolic dish system. Ray-tracing analysis has been performed with the open source software Tonatiuh, a ray-tracing tool specifically oriented to the modeling of solar concentrators.

Uma [**?**] carried out the simulation of the structural, thermal and CFD analysis of the dish with varying metallic properties (Aluminium, Copper and StainlessSteel) under different wind conditions. Computational Fluid Dynamics (CFD) was done to simulate the thermal performance of the dish at two different wind velocities.

Patil [**?**] described the development of automatic dual axis solar tracking system for solar parabolic dish. Five light dependent resistors were used to sense the sunlight and Two permanent magnet DC motors are used to move the solar dish. A controller software were developed to control the motors using the data sensed by the resistors.

Pavlovic [**?**] presented a procedure to design a square facet concentrator for laboratory-scale research on medium-temperature thermal processes. A parabolic collector made up of individual square mirror panels (facets) were investigated. These facets can deliver up to 13.604 kW radiative power over a 250 mm radius dish receiver with average concentrating ratio exceeding 1200.

1.2.3 Power tower

Besarati and Yogi [**?**] developed a new and simple method to improve the calculation speed and accuracy for shading and blocking computation of the heliostat field. The Sassi method [**?**] is used for the shading and blocking efficiency. A 50 MWth heliostat field in Dagget, California, USA was used as a case study for the proposed method.

Haroun [**?**] proposed a novel system combines both solar chimney and solar tower. The solar tower receiver was installed at the top of the chimney. Theoretical study of this novel system was conducted. The results shown that the new system generates more power than conventional system with the same parameters of solar irradiance, collector radius, height of chimney, and height of solar tower. The inlet air speed of the chimney is higher than that of the conventional, and it increases with the solar irradiance. Moreover, the results indicated that there exists a optimum ratio of solar tower height to solar chimney height for the maximum overall power.

Franchini et al. [**?**] developed a computing procedure for solar tower system under both nominal and part load conditions. A Siemens gas turbine product, SGT-800, was considered as a study case for the solar tower system. The turbine has a dual pressure heat recovery steam generator, which can be used for the Integrated Solar Combined Cycle (ISCC) plant. A model of Solar Rankine Cycle (SRC) driven by PTCs was also developed for comparison. A highest solar-to-electric efficiency of 21.8% can be achieved by the designed ISCC plant. And in all conditions, the global solar energy conversion efficiency of the ISCC is higher than that of the SRC. [C]ISCCIntegrated Solar Combined Cycle [C]SRCSteam Rankine Cycle

Kim et al. [**?**] investigated the heat loss of solar central receiver. Numerical simulations using CFD (Computational Fluid Dynamics) with the consideration of four different receiver shapes were carried out to get the influence on convection and radiation heat losses. Different opening ratio between cavity aperture area and receiver aperture area, receiver temperatures, wind velocities and wind directions (head-on and side-on) were considered for the simulations. Results were used to get a simplified correlation model which gets the fraction of convection heat loss. The correlation obtained showed good agreements with the simulation results. The correlation was also validated with experimental data from three central receiver systems (Martin Marietta, Solar One and Solar Two). [C]CFDComputational Fluid Dynamics

Lara et al. [**?**] presented a novel modeling tool for calculation of central re-

ceiver concentrated flux distributions. The modeling tool is based on a drift model that includes different geometrical error sources in a rigorous manner and on a simple analytic approximation for the individual flux distribution of a heliostat. The model is applied to a group of heliostats of a real field to obtain the resulting flux distribution and its variation along the day. The distributions differ strongly from those obtained assuming the ideal case without drift or a case with a Gaussian tracking error function. The time evolution of peak flux is also calculated to demonstrate the capabilities of the model. The evolution of this parameter also shows strong differences in comparison to the case without drift.

Wei et al. [**?**] proposed a new method for the design of the heliostat field layout for solar tower power plant. In the new method, the heliostat boundary is constrained by the receiver geometrical aperture and the efficiency factor which is the product of the annual cosine efficiency and the annual atmospheric transmission efficiency of heliostat. With the new method, the annual interception efficiency does not need to be calculated when places the heliostats, therefore the total time of design and optimization is saved significantly. Based on the new method, a new code for heliostat field layout design (HFLD) has been developed and a new heliostat field layout for the PS10 plant at the PS10 location has been designed by using the new code. Compared with current PS10 layout, the new designed heliostats have the same optical efficiency but with a faster response speed. In addition, to evaluate the feasibility of crops growth on the field land under heliostats, a new calculation method for the annual sunshine duration on the land surface is proposed as well.

Wei et al. [**?**] developed a new code for the design and analysis of the heliostat field layout for power tower system. In the new code, a new method for the heliostat field layout is proposed based on the edge ray principle of nonimaging optics. The heliostat field boundary is constrained by the tower height, the receiver tilt angle and size and the heliostat efficiency factor which is the product of the annual cosine efficiency and the annual atmospheric transmission efficiency. With the new method, the heliostat can be placed with a higher efficiency and a faster response speed of the design and optimization can be obtained. A new module for

the analysis of the aspherical heliostat is created in the new code. A new toroidal heliostat field is designed and analyzed by using the new code. Compared with the spherical heliostat, the solar image radius of the field is reduced by about 30% by using the toroidal heliostat if the mirror shape and the tracking are ideal. In addition, to maximize the utilization of land, suitable crops can be considered to be planted under heliostats. To evaluate the feasibility of the crop growth, a method for calculating the annual distribution of sunshine duration on the land surface is developed as well.

Xu et al. [**?**] created a model of the 1 MW Dahan solar thermal power tower plant using the modular modeling method. The dynamic and static characteristics of the power plant are analyzed based on these models. Response curves of the system state parameters are given for different solar irradiance disturbances. Conclusions in this paper are good references for the design of solar thermal power tower plant.

Xu et al. [**?**] built the thermal energy storage model of Badaling 1 MW solar power tower plant using the modular modeling method. This model can accurately simulate the recharge and discharge processes of thermal energy storage system. The dynamic and static characteristics of the thermal energy storage system are analyzed based on the model response curves of the system state parameters that are obtained from different steam flow disturbances. Conclusions of this paper are good references for the design, operating, and control strategy of solar thermal power plant.

1.2.4 Cascade solar system

1.2.4.1 Cascade collection

Suzuki [**?**] analyzed the solar thermal systems with two different types of collectors connected in series. A key value of the collectors was revealed to be the key factor to determine whether a cascade system is better than either one of the collectors alone. The value is the product of the collector efficiency factor and the optical efficiency. If the value of the lower concentration ratio collector is lager

than that of the higher concentration ratio, the cascade system is more effective. Furthermore, to obtain the maximum energy gain, there exists the optimum operating conditions.

Oshida and Suzuki [**?**] presented the idea of optical cascade heat collection of solar energy. Two absorbers, one warm and the other hot, are used in the cascade system. The warm absorber is heated by the Fresnel lenses and the hot absorber is heated by CPC. HTF flows into the warm absorber firstly and then flows into the hot absorber. The temperature of HTF can increase more effectively. [C]CPCCompound parabolic collector

Kribus et al. [**?**] proposed an idea of using separate aperture stages for different irradiance distribution.

A high-temperature solar thermal receiver is subject to temperature-dependent emission and convection losses. Minimizing these losses is essential to realization of high temperature, high efficiency systems. Dividing the aperture into separate stages according to the irradiance distribution has been shown theoretically to significantly reduce these losses. In such a partitioned system, the working fluid is gradually heated as it passes through a sequence of receiver elements with increasing irradiance levels. An experiment to demonstrate this principle using two heating stages has been constructed at the Weizmann Institute' s Solar Tower. The high-temperature receiver stage is the Directly Irradiated Annular Pressurized Receiver (DIAPR). The low-temperature stage is implemented as a partial ring of intermediate-temperature cavity tubular receivers (Preheaters) surrounding the central high-temperature stage. Following initial concentration by a part of the Weizmann Institute heliostat field, the light enters the receivers via secondary concentrators constructed as approximate CPCs. We present recent test results with the two-stage system. Air exit temperatures of up to 1000°C were obtained, with the low-temperature stage supplying up to 750°C. The power output was up to 55 kWth. Heat transfer in the high-temperature receiver, losses due to the partitioning, and future plans for partitioned receivers are discussed.

Collado2016 and Guallar [**?**] proposed a method breaking the optimization process of solar power tower system down into two consecutive steps. First, a pri-

mary, or energy, optimization, which is practically independent of the cost models, and then a main, or economic, optimization. The primary optimization seeks a heliostat layout supplying the maximum annual incident energy for all the explored combinations of receiver sizes and tower heights. The annual electric output is then calculated as the combination of the incident energy and the simplified (annual averaged) receiver thermal losses and power efficiencies. Finally, the figure of merit of the main optimization is the levelized cost of electric energy (LCOE) where the capital cost models used for the LCOE calculation are reported by the System Advisor Model (SAM)-NREL and Sandia. This structured optimization, splitting energy procedures from economic ones, enables the organization of a rather complex process, and it is not limited to any particular power tower code. Moreover, as the heliostat field layout is already fully optimized before the economic optimization, the profiles of the LCOE versus the receiver radius for the tower heights explored here are sharp enough to establish optima easily. As an example of the new procedure, we present a full thermo-economic optimization for the design of the collector field of an actual SPT system (Gemasolar, 20 MWe, radially staggered surrounding field with 2650 heliostats, 15 h of storage). The optimum design found for Gemasolar is reasonably consistent with the scarce open data. Finally, optimum designs are strongly dependent on the receiver cost, the electricity tariff and the assumed maximum receiver surface temperature.

Reddy [**?**] carried out the numerical analysis of solar dish modified cavity receiver with Cone, CPC and Trumpet reflectors is presented. Three-dimensional modeling to estimate the convective and radiative heat loss from the receiver for different angles of inclination and operating temperatures. Incorporating reflectors in the modified cavity receiver for second stage concentration, the natural convection heat losses are reduced by 29.23, 19.81 and 19.16%, respectively. The receiver with the trumpet reflector has shown better performance as compared to other configurations.

Gordon and Saltiel [**?**] presented an analytic method for predicting the long-term performance of solar energy systems with more than one collector brand (“multi-stage” systems). This procedure enables the designer to determine the

most cost-effective method of combining different collector brands for a given load. Although our derivations pertain to solar systems for constant load applications and/or near constant collector operating threshold, they can also be used for conventional multi-pass designs. The problems of excess energy delivery, and of various collector on/off control strategies, are taken into account. Our results are simple closed-form expressions whose evaluation requires readily-available average climatic data, and load and collector characteristics. The analytic method is illustrated by a solved example which shows that significant savings can be realized by combining different collector brands for a given application (multi-staging).

Good et al. [**?**] proposed an entirely novel solar receiver design for solar trough concentrators using air as heat transfer fluid at operating temperatures exceeding 600 °C. It consists of an array of helically coiled absorber tubes contained side-by-side within an insulated groove having a rectangular windowed opening. Secondary concentrating optics are incorporated to boost the geometric concentration ratio to 97×. The multiple absorber tubes are connected via two axial pipes serving as feeding and collecting manifolds. The steady-state energy conservation equation coupling radiation, convection, and conduction is formulated and solved numerically using the finite volume technique. The solar flux distribution incident at each absorber tube is determined by Monte Carlo ray-tracing using spectrally and directionally dependent optical properties. Thermal radiative heat exchange is analyzed using the gray-band approximated radiosity method for an enclosure with a selective window. Model validation is accomplished by comparison to on-sun experiments with a 1 m-long solar receiver prototype composed of 7 absorber tubes, mounted on a 4.85 m-aperture solar trough concentrator. Feeding rates in the range of $5^{-}20$ ln/min to each absorber tube led to air outlet temperatures of 621–449 °C and a peak receiver efficiency of 64%.

Barder et al. [**?**] developed a numerical model of a tubular cavity-receiver that uses air as the heat transfer fluid using a validated heat transfer model. The receiver is designed for use on a large-span (9 m net concentrator aperture width) solar parabolic trough concentrator. Through the combination of a parabolic primary concentrator with a nonimaging secondary concentrator, the collector reaches a

solar concentration ratio of 97.5. Four different receiver configurations are considered, with smooth or V-corrugated absorber tube and single- or double-glazed aperture window. The collector's performance is characterized by its optical efficiency and heat loss. The optical efficiency is determined with the Monte Carlo ray-tracing method. Radiative heat exchange inside the receiver is calculated with the net radiation method. The 2D steady-state energy equation, which couples conductive, convective, and radiative heat transfer, is solved for the solid domains of the receiver cross-section, using finite-volume techniques. Simulations for Sevilla/Spain at the summer solstice at solar noon (direct normal solar irradiance: 847 $\mathrm{W{\cdot}m^{-2}}$, solar incidence angle: 13.9°) yield collector efficiencies between 60% and 65% at a heat transfer fluid temperature of 125°C and between 37% and 42% at 500°C, depending on the receiver configuration. The optical losses amount to more than 30% of the incident solar radiation and constitute the largest source of energy loss. For a 200 m long collector module operated between 300 and 500°C, the isentropic pumping power required to pump the {HTF} through the receiver is between 11 and 17 kW.

Some researchers have investigated the combination of different types of collectors for CSP. Desai et al. [**?**] presented an integrated CSP plant configuration with the combination of both PTC and LFC. Thermo-economic comparisons between PTC-based, LFC-based and integrated CSP plant configurations, without hybridization and storage, were analyzed. It is demonstrated that the cost of energy of an integrated CSP plant is $9.6\,\%$ cheaper than PTC-based CSP plant and $13.5\,\%$ cheaper than LFR-based CSP plant. Coco et al. [**?**] developed four different line-focusing solar power plant configurations integrated both direct steam generation and Brayton power cycle. In these configurations, collectors are divided into different solar fields to supply different heat demands. This provides the ability to use different types of collectors (parabolic trough and linear Fresnel) in the systems. [C]SRCSteam Rankine Cycle [C]ISCCIntegrated Solar Combined Cycle

1.2.4.2 Cascade utilization

Many researchers have done the work on the combination of different thermodynamic cycles for CSP. Lots of the work focused on integrated solar combined cycle (ISCC) with parabolic trough, where Rankine cycle is used as the bottom cycle. Li and Yang [**?**] proposed a novel two-stage ISCC system that could reach up to 30% of the net solar-to-electricity efficiency. In their research, the impact on the system overall efficiencies of how and where solar energy is input into ISCC system was investigated. Behar et al. [**?**] reviewed the R&D activities and published studies since the introduction of such a concept in the 1990s. One of the conclusions is that the higher the solar radiation intensity the better is the performance of the ISCCS than those of conventional CSP technologies. Gulen [**?**] used the exergy concept of the second law of thermodynamics to distill the complex optimization of ISCCS to its bare essentials. After the exergy analysis, physics-based, user-friendly guidelines were provided to help direct studies involving heavy use of time consuming system models in a focused manner and evaluate the results critically to arrive at feasible ISCC designs. Shaaban [**?**] introduced a novel ISCC with steam and organic Rankine cycles. The ORC was used in order to intercool the compressed air and produce a net power from the received thermal energy. The proposed cycle performance was studied and optimized with different ORC working fluids. Alqahtani and Dalia [**?**] quantified the economic and environmental benefits of an ISCC power plant relative to a stand-alone CSP with energy storage, and a natural gas-fired combined cycle plant. Results show that integrating the CSP into an ISCC reduces the LCOE of solar-generated electricity by 35-40% relative to a stand-alone CSP plant, and provides the additional benefit of dispatch ability. Manente [**?**] developed a 390 MWe three pressure level natural gas combined cycle to evaluate different integration schemes of ISCC. Both power boosting and fuel saving operation strategies were analyzed in the search for the highest annual efficiency and solar share. Result shown that, compared to power boosting, the fuel saving strategy shows lower thermal efficiencies of the integrated solar combined cycle due to the efficiency drop of gas turbine at re-

duced loads. Rovira et al. [**?**] compared the annual performance and economic feasibility of ISCC using two solar concentrating technologies: parabolic trough collectors (PTC) and linear Fresnel collectors (LFC). Different configurations were considered and results shown that only evaporative configuration is the most suitable choice. [C]PTCParabolic Trough Collector [C]LFCLinear Fresnel Collector Compared with traditional ISCC design, two new conceptual hybrid designs for ISCC with parabolic trough were represented by Turchi et al. [**?**]. In the first design, gas turbine waste heat is supplied for both heat transfer fluid heating and feed water preheating. In the second design, gas turbine waste heat is supplied for a thermal energy storage system. Mukhopadhyay and Ghosh [**?**] presented a conceptual configuration of a solar power tower combined heat and power plant with a topping air Brayton cycle. The conventional gas turbine combustion chamber is replaced with a solar receiver. A simple downstream Rankine cycle with a heat recovery steam generator and a process heater have been considered for integration with the solar Brayton cycle. Li et al. [**?**] presented a novel cascade system using both steam Rankine cycle (SRC) and organic Rankine cycle (ORC). Screw expander is employed in the steam Rankine cycle for its good applicability in power conversion with steam-liquid mixture. The heat released by steam condensation is used to drive the ORC. [C]ORCOrganic Rankine Cycle Al-Sulaiman [**?**] compared the produced power of an SRC-ORC combined cycle with traditional SRC cycle. The SRC is driven by parabolic trough solar collectors, and the ORC cycle is driven by the condensation heat of the SRC. Bahari et al. [**?**] considered the optimization of an integrated system using organic Rankine cycle to utilize the heat released by the Stirling cycle. However, the integrated system is a primitive design and it didn't consider the application in CSP field.

1.3 Research content

The research is based on the national cooperation project "Collaborative research on key technologies to produce electricity by cascade utilization solar thermal energy" as the background. The objective of this project is to research the

equipment of solar thermal power generation system, to propose, develop and optimize a solar thermal cascade system depending on the advantages and disadvantages of the solar thermal power generation systems, and to explore a new feasible technology for large-scale solar thermal power generation. The main contents and conclusions of this paper are as follows:

Firstly, mechanism models were established for the components of solar thermal power generation system. The mechanism mathematical models were developed according to the operation mechanism of the target object and physical equations. The key components in the system, such as collectors, steam generating system, steam turbine and Stirling engine, were modeled with details. The mathematical model of each component is a model verified by the classical theory or a large number of experimental data, which is the basic of the model of the cascade solar thermal power generation system. Heat loss models were established for the receivers of trough collector and dish collector. For the Stirling engine, based on the reasonable simplification and hypothesis, the model of the Stirling machine considered various losses and irrevisibilities was developed. The component models were developed in MATLAB by using object-oriented method. It makes full use of inheritance and polymorphism to ensure both the independence and the relevance of the components.

Secondly, the topological structure of solar thermal cascade power generation system was proposed. According to the analysis of thermal characteristics and the working characteristics of each component in the system, rationally arranged topological structures of cascade system were proposed. These systems use different thermodynamic cycles to utilize energy in different temperature zones. A reasonable cascade generation system can make full use of the mechanism models of the power generation system and provide the foundation for higher efficiency solar thermal cascade generation systems. In this paper, several schemes of feasible topological structures of solar thermal cascade system were set up according to the mechanism model of each component. After system evaluation, parameter selection, preliminary calculation and scheme comparison, two representative typical schemes were determined. In one scheme, both Rankine cycle (water as the work-

ing fluid) and Stirling cycle are used for power generation. Cooling water of the Rankine cycle is used to cool the hot end of the Stirling engines to recover the released heat. In the other scheme, multiple organic Rankine cycles are used for power generation. Condensation heat of upper cycle is absorbed by lower cycle for energy cascade utilization.

Thirdly, the solar thermal cascade generation system models were developed. Based on the selected solar thermal cascade generation systems, solar thermal cascade generation system models were established based on the model of each component in the systems. The object-oriented features of inheritance, combination and polymorphism were used for the model development. The change rules of the main parameters and the performance indexes under the coupling of external and internal factors were studied. The change mechanism was studied and the calculation method of its performance characteristics was established. After setting up the components, setting the parameters and compiling the environment, the paper completes the system construction of each system scheme, and finally completes the simulation system of solar thermal cascade generation based on MATLAB with the copyright of independent computer software. The system components are relatively independent, easy to replace or improve the parts model; the results of the calculation of the system model can be a single object to easily view the various components of the system key parameters.

Then, simulation and optimization of cascade solar thermal power generation system model. Based on the study of the performance characteristics of solar thermal cascade generation system, the system is optimized and the structure is reconstructed. In particular, by analyzing the steam generation system of the system, a method of staged heating is proposed to reduce the heat transfer temperature difference in the steam generating system by changing the mass flow rate of the heat conduction oil, effectively reducing the heat generated during the heat exchange process in the steam generating system. Which can improve the efficiency of the whole system. Based on Stirling unit in cascade system, five kinds of basic arrangement forms of Stirling unit are summarized, and the difference of unit efficiency and output power under various arrangement forms is analyzed, and a given cold

and heat source fluid Stirling unit under the conditions of the best arrangement.

Finally, the operating parameters of solar thermal cascade power generation system are optimized. According to the specific structural scheme and operation mode, the performance parameters and economic indexes of the cascade generation system are taken as the objective function, reasonable adjustable parameters are selected, various constraints are established, and modern optimization methods such as genetic algorithm and ant colony algorithm are used to complete the system Parameter optimization analysis, as well as the independent system for comparative analysis. The results show that solar thermal cascade power generation system has higher overall photoelectric conversion efficiency under certain parameter conditions than its corresponding independent system. Under the condition of direct solar radiation intensity of $700\,\mathrm{W/m^2}$ and dish type collector outlet air temperature of 800°C, the solar thermal cascade power generation system of Scheme 1 is better than the corresponding The efficiency of stand-alone system is increased by 5.2%. The solar thermal cascade power generation system selected in Scheme 2 is 15.3% more efficient than the corresponding independent system.

footnotefootnote # Chapter 2

System topology

2.1 System topology design

2.1.1 Basic systems

The objective of this research is to research the equipment of solar thermal power generation system, to propose, develop and optimize a solar thermal cascade system depending on the advantages and disadvantages of the solar thermal power generation systems. The research is based on the national cooperation project "Collaborative research on key technologies to produce electricity by cascade utilization solar thermal energy" as the background. There are three kinds of mature technologies been applied commercially – parabolic trough, parabolic dish and solar tower. Considering the future deployment of solar cascade demo system, two solar thermal technologies, parabolic trough and parabolic dish, are chosen as the basic systems for the design of cascade solar thermal power system. For the cascade utilization of the high temperature of the parabolic receiver, air (or nitrogen) is used as the HTF to transfer the heat collected. Figure

With different considerations (such as water Rankine cycle or ORC, combination of different systems, connection types of collectors, etc) of the cascade system topology, multiple combination topologies may be used for cascade systems. To get the most suitable system topology, these considerations will be analyzed in the following sections.

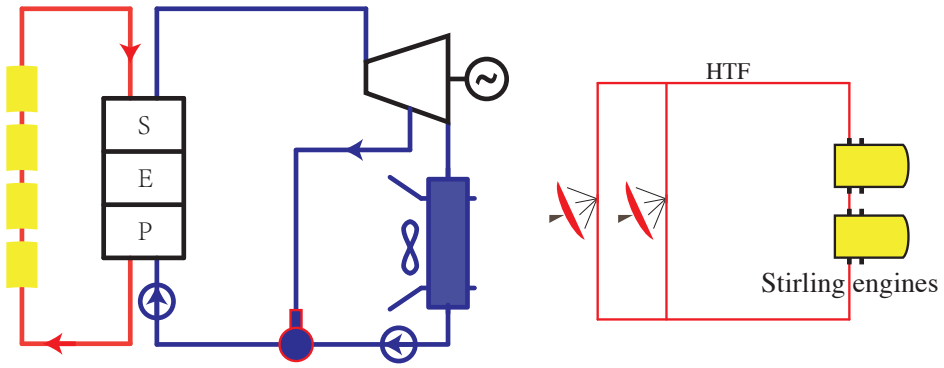

Figure 2.1: Schematic diagrams of a parabolic trough system and a parabolic dish system

2.1.2 Rankine cycle fluid

An ideal working fluid would have the temperature entropy diagram given in Fig

Water is the most commonly used fluid for Rankine cycle, it is mare mature to design Rankine cycle components for steam systems than any other liquid. It is inexpensive to use (although boiler-grade water must be highly distilled and thus costs more than tap water), sealing of the high-pressure portions of a Rankine cycle using steam is not critical. Non-flammability and ready availability of steam are additional advantages. Because it has a critical temperature and pressure of $374\,^{\circ}\mathrm{C}/22.1\,\mathrm{MPa}$, it can be used for systems operating at fairly high temperatures with most of the heat addition (at constant temperature) and at moderate pressure. Figure

There are some disadvantages for steam as the Rankine cycle fluid. The low temperature characteristics of steam are not ideal because the steam has a low vapor pressure (see table

The organic Rankine cycle can be used in the solar parabolic trough technology in place of the usual steam Rankine cycle. The ORC allows power generation

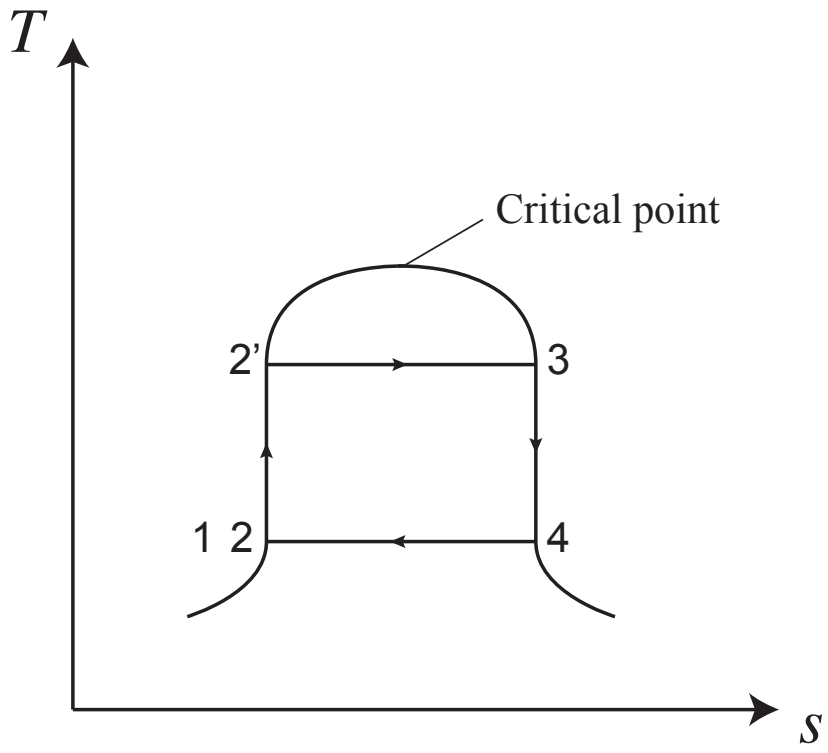

Figure 2.2: Collector and Rankine cycle efficiency variation with operating temperature

at lower capacities and with a lower collector temperature, and hence the possibility for low-cost, small scale decentralized CSP units. Most organic fluids used in organic Rankine cycle are drying fluids. The vapor leaving the expander still contains heat that can be transferred to the compressed liquid stream because the turbine outlet temperature is above the condenser temperature. A vapor-to-liquid heat exchanger, known as a regenerator, is typically used for this purpose. Fig.

Compared with steam for the Rankine cycle, it has the following advantages:

- Small turbine head allows for moderate shaft speed and a single- or two-stage design.
- Low volume ratio facilitates the flow path design.
- High volume flow and low velocity of sound results in reasonable flow areas.
- Low temperature drop during expansion reduces thermal stress problems.

[b]0.4

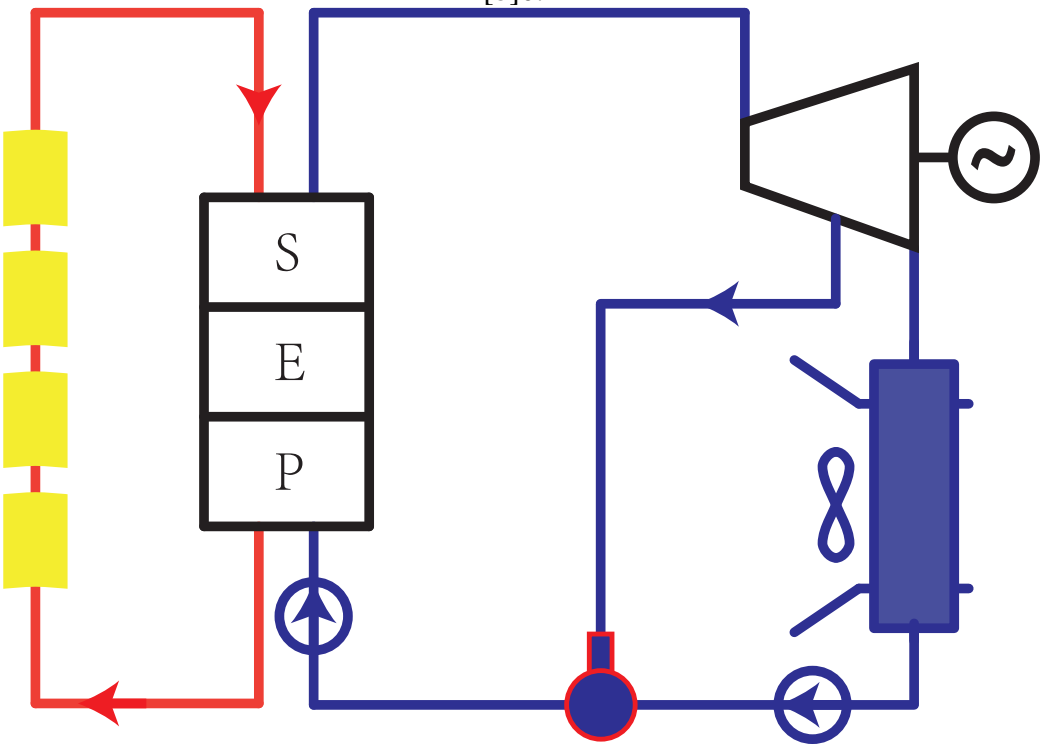

Figure 2.3:

[b]0.4

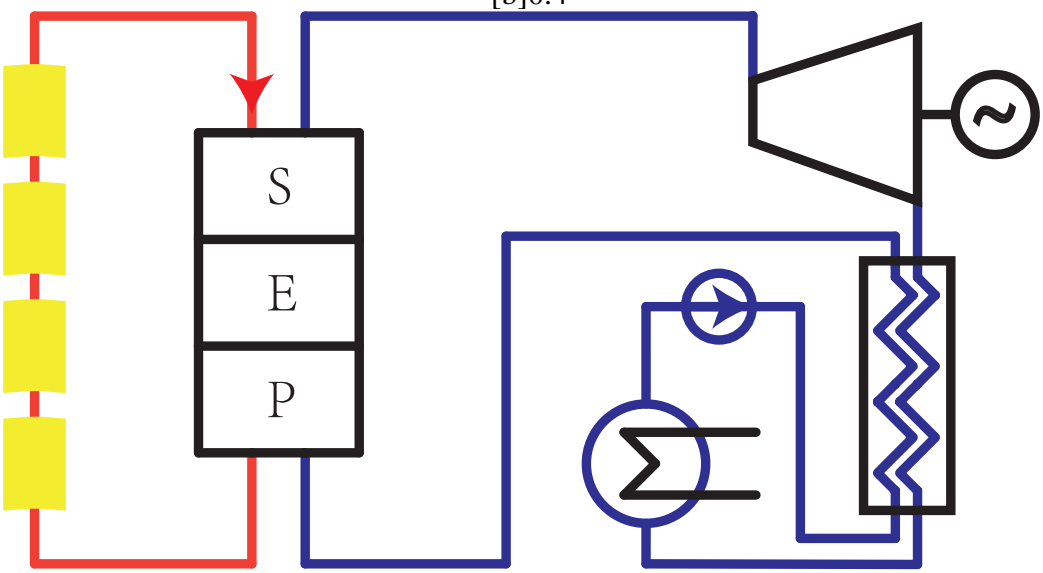

Figure 2.4:

Figure 2.5: Schematic diagrams of two types of Rankine cycle solar system

- Dry expansion avoids blade erosion caused by vapor wetness.
- Low system pressure facilitates housing design.

2.1.3 Solar chimney

Solar chimney, also known as solar updraft tower, directly (without concentration) uses the sun's heat to generate power. It uses solar radiation to increase the internal air temperature to form a flow to the chimney located at the middle of the roof. Fig.

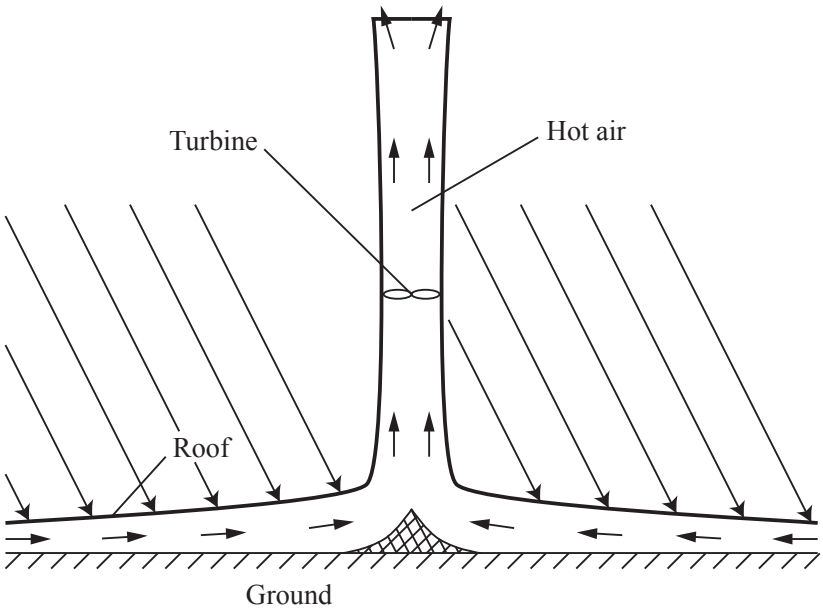

Figure 2.6: Schematic diagram of a solar chimney power plant

The solar chimney can use the low temperature (low grade energy) for power generation. So the combination of parabolic trough system and solar chimney is considered an effective way for energy cascade utilization. In the combined system, the condenser in the Rankine cycle is air cooled. The fan blows the hot air that has cooled the condenser into the solar chimney power plant from its periphery. The hot air stream converges at the bottom of chimney, flows upward with the action of buoyancy and drives the turbine in the chimney. Energy of the hot air can be utilized by the solar chimney. Fig.

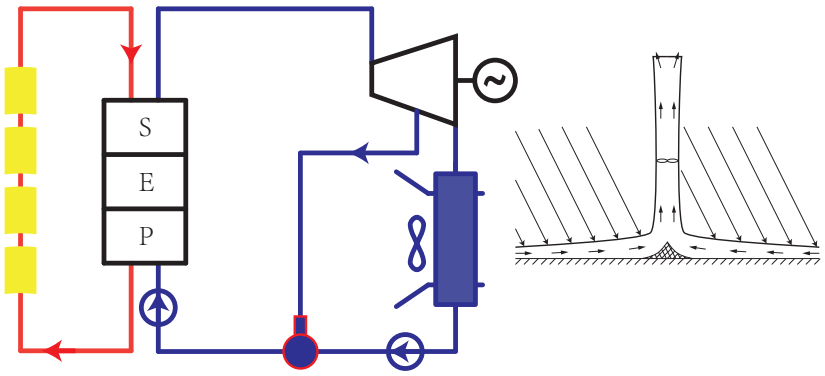

Figure 2.7: Schematic diagram of a combined solar trough and chimney power system

2.1.4 Collector series connection

Considering different heat collecting temperatures of different types of collectors, series connection of different types of collectors can be a feasible choice for solar cascade collection. Trough collectors and Fresnel collectors have better performance for lower temperature heat collection. Dish collectors and solar towers are more suitable for higher temperature heat collection. Serial connection utilize the advantages of different types of collectors. Figure

2.1.5 Direct steam generation

All commercial parabolic trough solar plants implemented to date use heat-transfer fluid (typically synthetic oil or melton salt) in the solar field. It leads to high pressure drop, limits the oil (or salt) related equipment operation, maintenance and cost. Besides, the highest temperature of the Rankine cycle is limited by the oil (or salt) temperature. So generating steam in the receiver tubes (direct steam generation, DSG) of the solar collector is one of the directions to reduce the cost and increase the efficiency of the PTC systems. Fig.

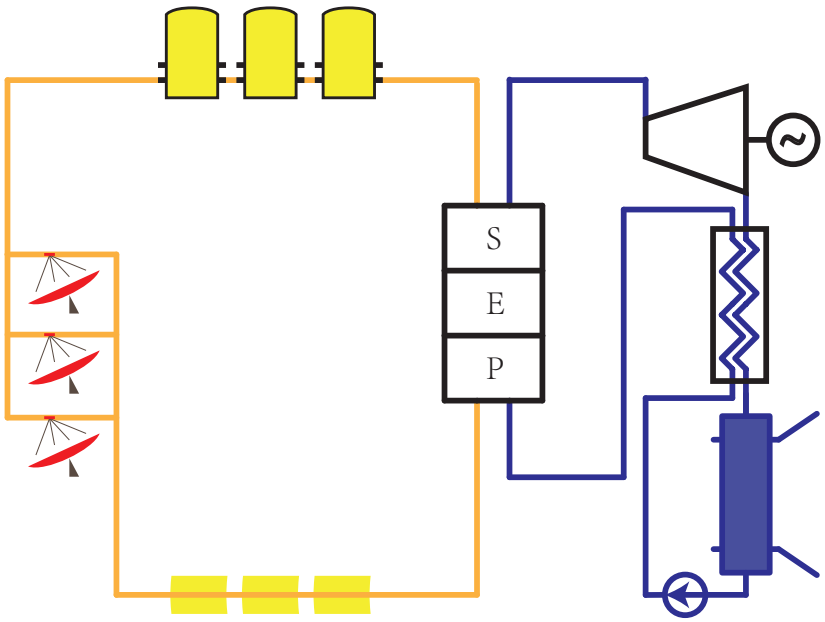

Figure 2.8: Schematic diagram of a cascade system using collector series connection

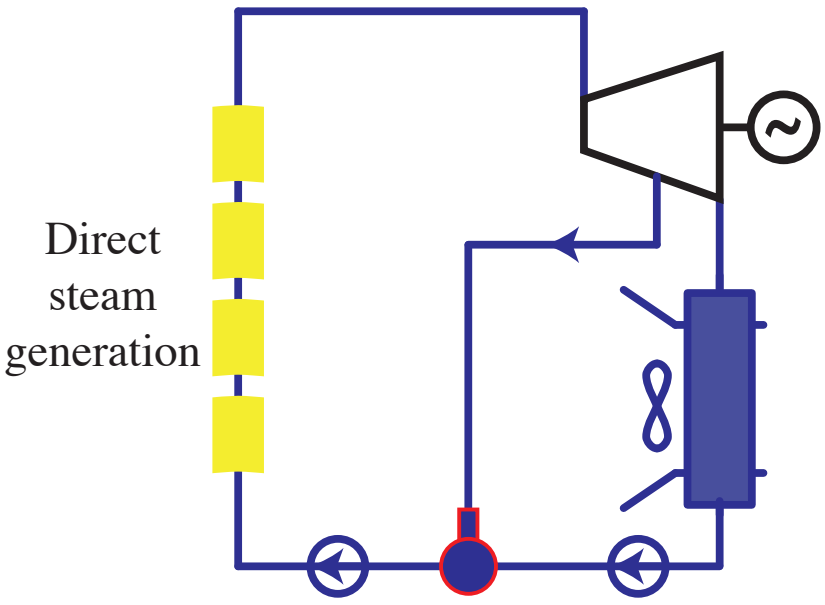

Figure 2.9: schematic diagram of a typical solar system using receiver vapor generator

2.1.6 Heat exchanger between circuits

Heat transfer between different circuits can be applied for cascade utilization of the heat collected. Depending on the two basic solar system in

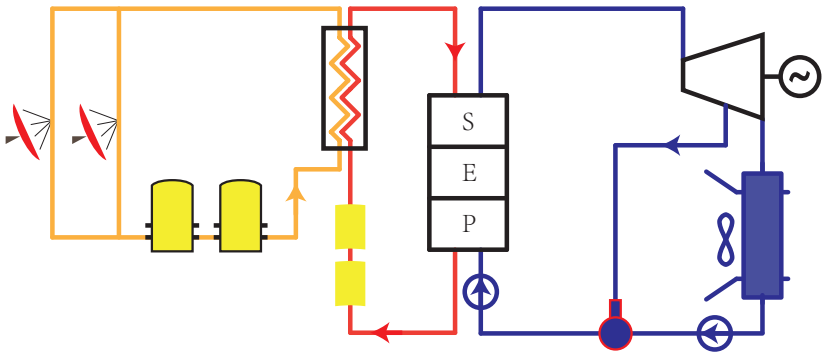

Figure 2.10: Schematic diagram of a solar system using air-oil heat exchanger

In the second type, air-water heat exchanger is applied to transfer heat between the air circuit and the oil circuit. Figrue

2.1.7 Heat recovery between cycles

According to the second law of thermodynamics, it is impossible for any device that operates on a cycle to receive heat from a single reservoir and produce a net amount of work. For a heat engine, it requires both a hot source and a cold sink to convert heat energy to mechanical energy. Fig

Engines that only suitable for external heating are usually considered for solar applications. Unlike an internal combustion engine that generates heat within the working fluid, an externally heated engine needs external heat to be added to the working fluid by a heat exchanger.

Three types of engines are designed to accept external heat and have been used for solar heat sources: the Rankine, the Stirling, and the Brayton cycles [**?**]. The Rankine and Brayton cycles are both suitable for constant-pressure heat-addition. The original Brayton engine uses piston compressors and piston expanders, but more modern gas turbines and airbreathing jet engines also follow the Brayton cycle. Although the cycle is usually an open system, in order to carry out thermodynamic analysis, usually it is assumed that exhaust gases are reused as the intake so that the whole process can be analyzed as a closed cycle. The Stirling machine

[b]0.4

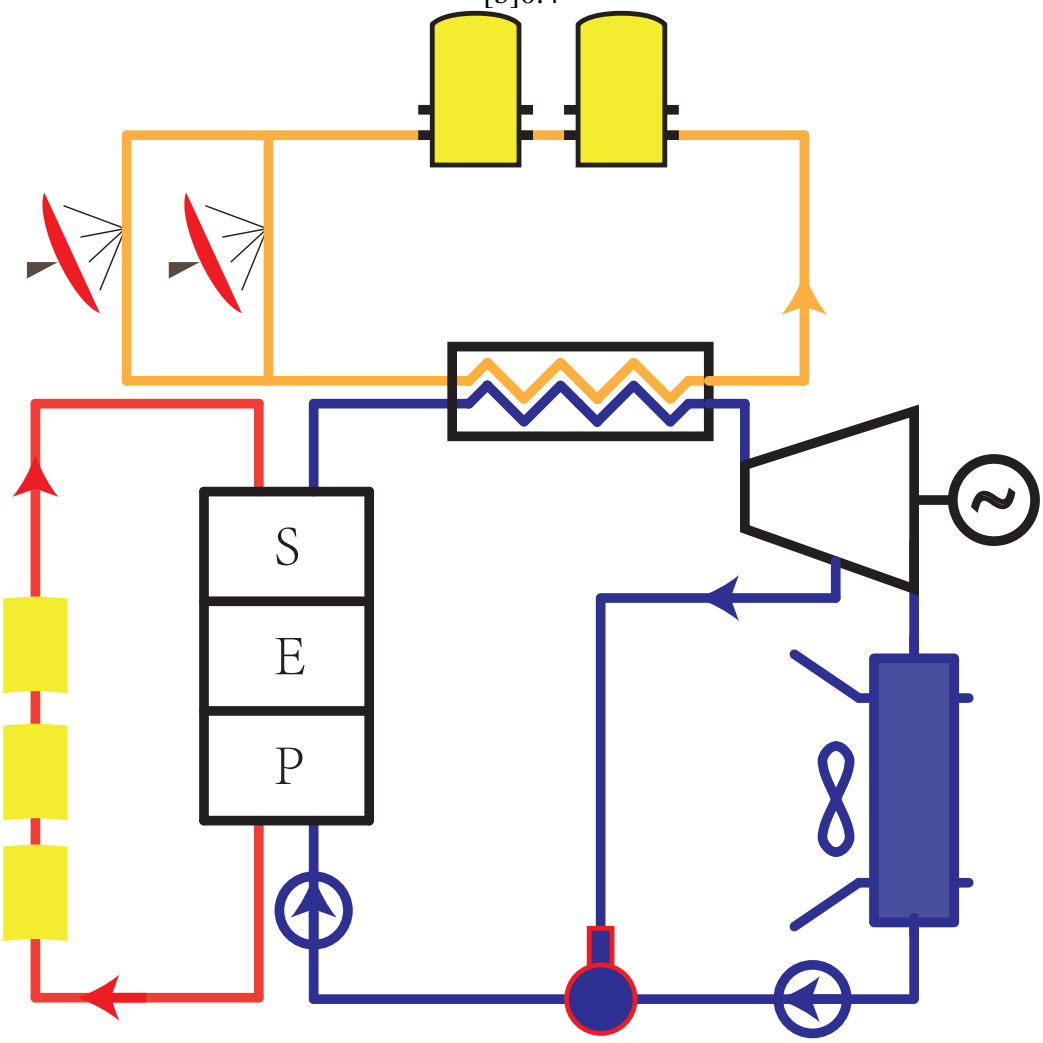

Figure 2.11:

[b]0.4

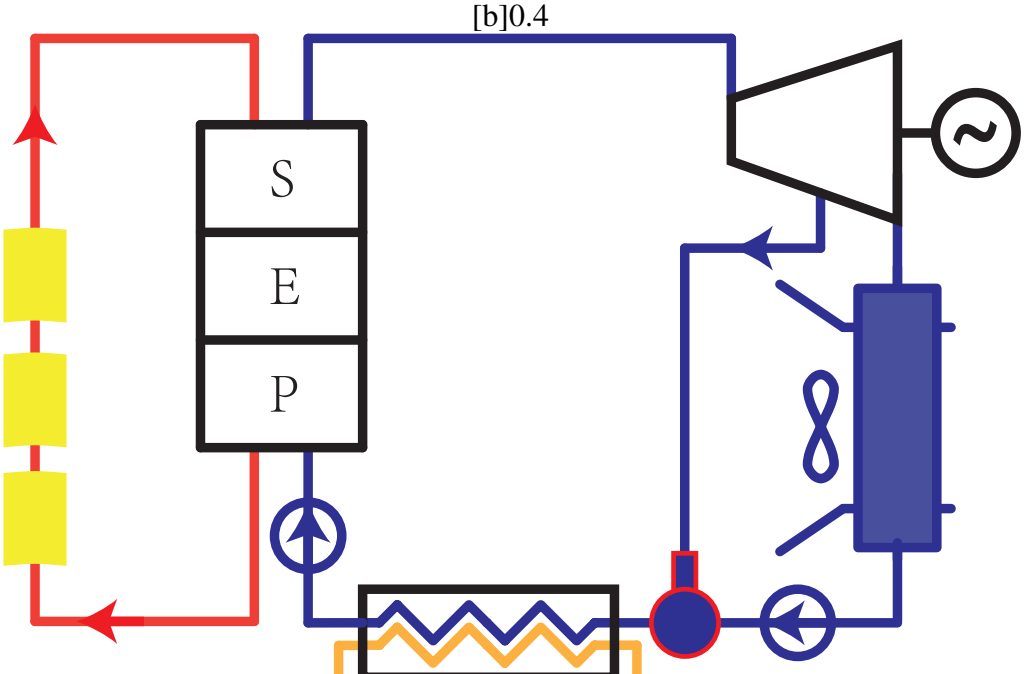

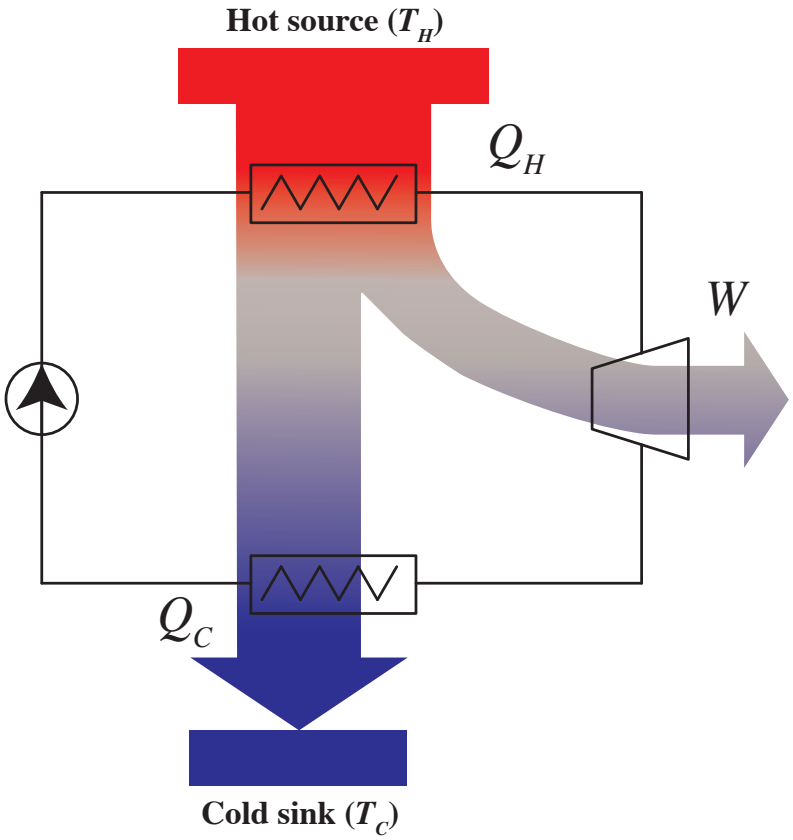

Figure 2.14: Diagram of a typical heat engine

uses a reciprocating piston design that allows external heating to be combined into its constant-temperature heat-addition process. In a Rankine cycle, the pressurized liquid enters a boiler (or a heat exchanger) where it is heated at constant pressure by an external heat source to become a dry saturated vapor.

These three kinds of cycles work at different optimum operating temperatures. Rankine cycle works with the lowest hot source temperature and Brayton works with the highest. Figure

Dunham [**?**] proposed a single Brayton and a combined Brayton-Rankine power cycle for distributed solar power generation and compared its theoretical efficiency to a single Brayton cycle. In the combined power cycle, exhaust gas of the turbine is used to provide heat for Rankine cycle. Working fluids including air, Ar, CO_2, He, H_2, and N_2 are examined for the topping Brayton cycle. C6-fluoroketone,

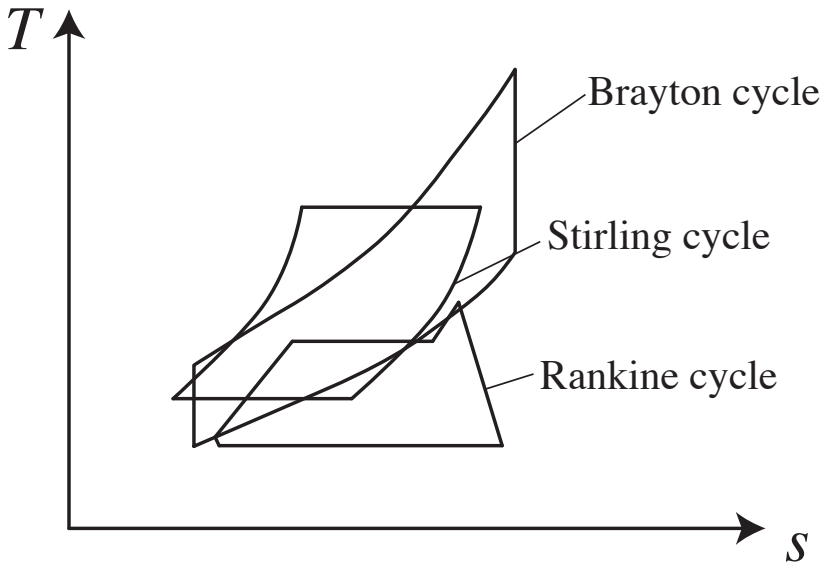

Figure 2.15: Diagram of three cycles used in solar energy

cyclohexane, n-pentane, R-141b, R-245fa, and HFE-7000 are examined as working fluids in the bottoming Rankine cycle. It is found that the combination of the Brayton topping cycle using carbon dioxide and the Rankine bottoming cycle using R-245fa gives the highest combined cycle efficiency of 21.06%, while a single Brayton cycle is found to reach a peak cycle efficiency of 15.31% with carbon dioxide at the same design point conditions.

Bahrami et al. [**?**] proposed a combined Stirling-organic Rankine cycle (ORC) power cycle. An ORC was used as the cold-side heat rejector of a Stirling engine. The operating temperatures of the ORC are between 80 °C and 140 °C and the combined system can achieve 4% to 8% higher efficiency compared with a standard Stirling cycle.

Li et al. [**?**] proposed a novel solar electricity generation system (SEGS) using both SRC and ORC. Screw expander (SE) is employed in the SRC for its good applicability in power conversion with steam-liquid mixture. The heat released by steam condensation is used to drive the ORC. Simulation results show that efficiency of 13.68−15.62% for the proposed system can be achieved.

Thierry et al. [**?**] proposed a nonlinear optimization formulation of multistage

Rankine cycle with two types of configurations. Both cascade style and series style of the ORC are considered. The results show that for some cases the multistage configurations can achieve higher efficiency at low temperature.

In our basic systems (see section

2.2 System topology selection

2.2.1 Rankine cycle fluid

There are two important aspects to consider when selecting the working fluid of the Rankine cycle solar power system:

1. Select the working fluid that is conducive to the optimization of the cycle efficiency

   For a Rankine cycle solar system, the collector efficiency reduces with operating temperature, and the Rankine cycle efficiency increases with operating temperature, there exists an optimal operating temperature as illustrated in Fig.

2. The working fluid state matches the heat transfer fluid state, if heat transfer fluid is used.

   On the one hand, the operating temperature of the working fluid should be lower than the collecting temperature of the HTF. On the other hand, the operating temperature of the working fluid should not be much lower than the collecting temperature of the HTF to avoid large exerge loss during the heat exchange process.

Based on the advantages and disadvantages of water and organic fluid as the working fluid of Rankine cycle, it is clear that, for low operating temperature and small capacity distribution power generation, organic fluid will be a better choice, otherwise water is the better one. Bao and Zhao [**?**] presented a comprehensive review of working fluid selection (including pure fluids and mixtures). In this review, many factors such as operating conditions, working fluid characteristics,

[b]0.4

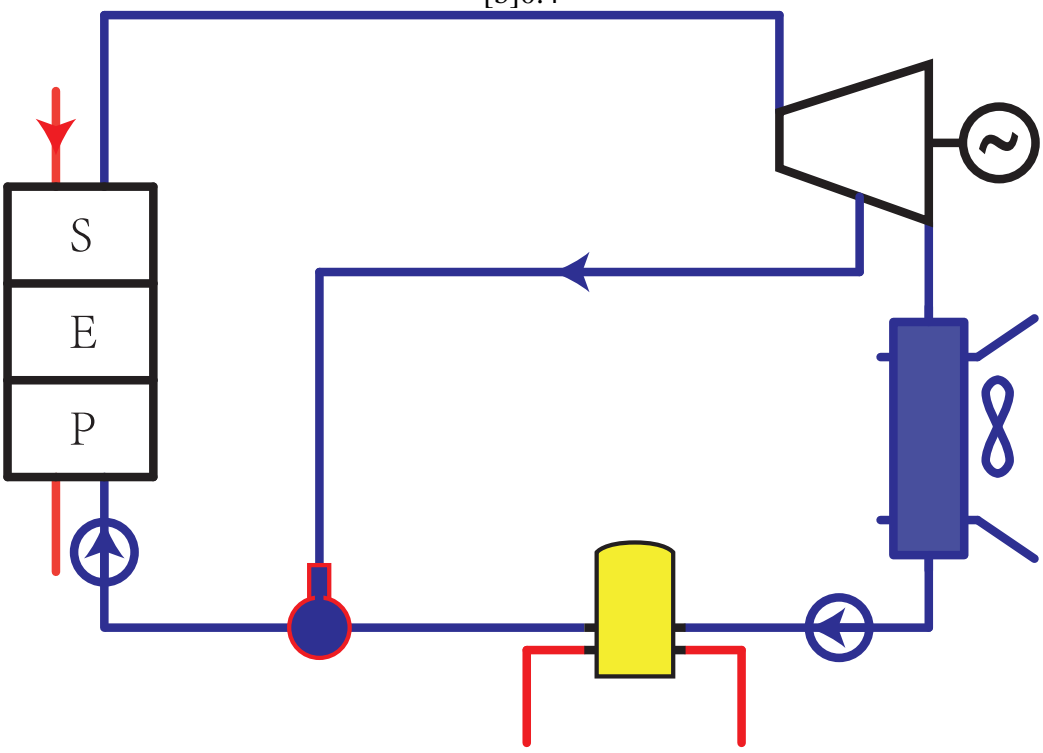

Figure 2.16:

[b]0.4

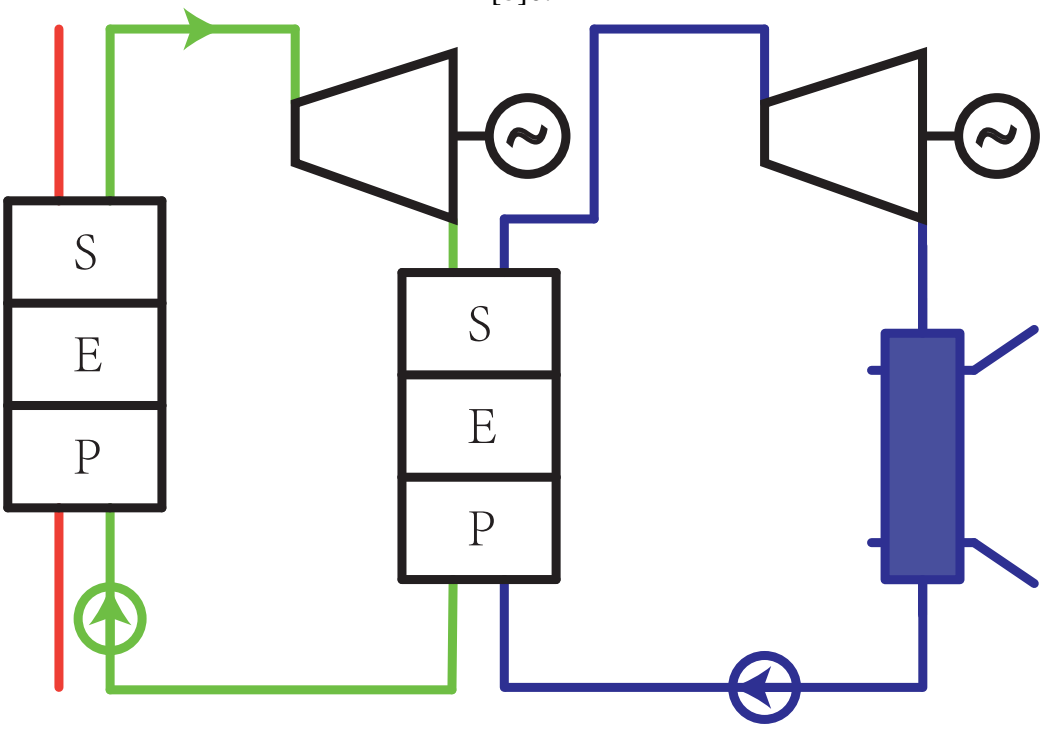

Figure 2.17:

Figure 2.18: Schematic diagrams of two kinds of solar systems using air-water heat exchanger

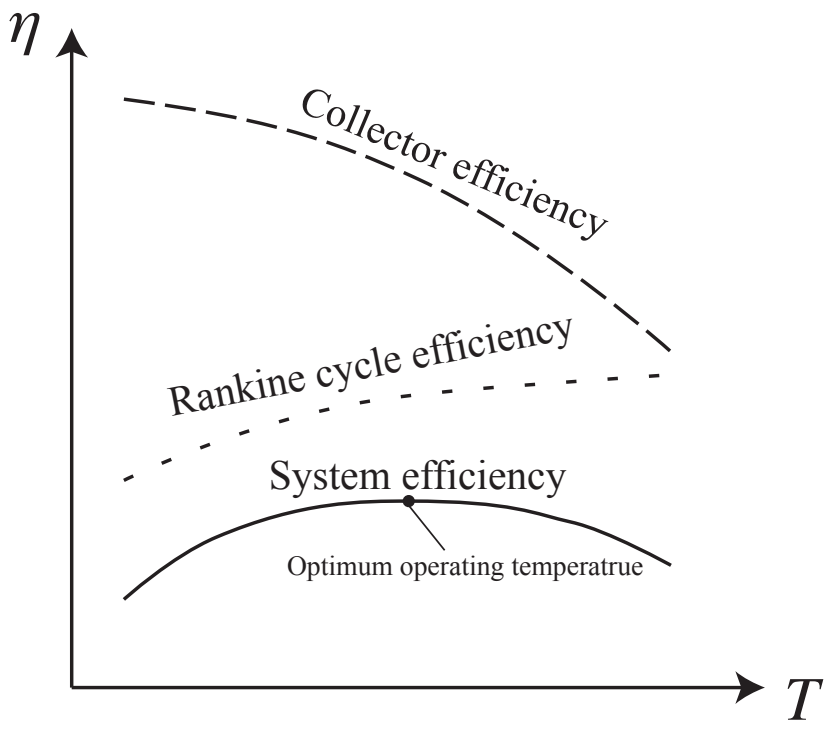

Figure 2.19: Collector and Rankine cycle efficiency variation with operating temperature

equipment structures and environmental safety considerations were considered. It has to be mentioned that the types of working fluids (mainly dry or wet) will affect the operation and layout of the system.

2.2.2 Solar chimney

Section

Besides, a solar chimney is costly and requires vast land, which is adverse to the future deployment of solar cascade demo system. With these considerations, the solar chimney plans are not adopted.

2.2.3 Collector series connection

Each type of collector has its own suitable temperature range. It is feasible to heat the HTF step by step using different types of collectors with series connection.

It can be a good choice to apply flat plate solar collectors and parabolic trough collectors in traditional solar tower power plant that uses water as the HTF (such as Solar One). As demonstrated in fig.

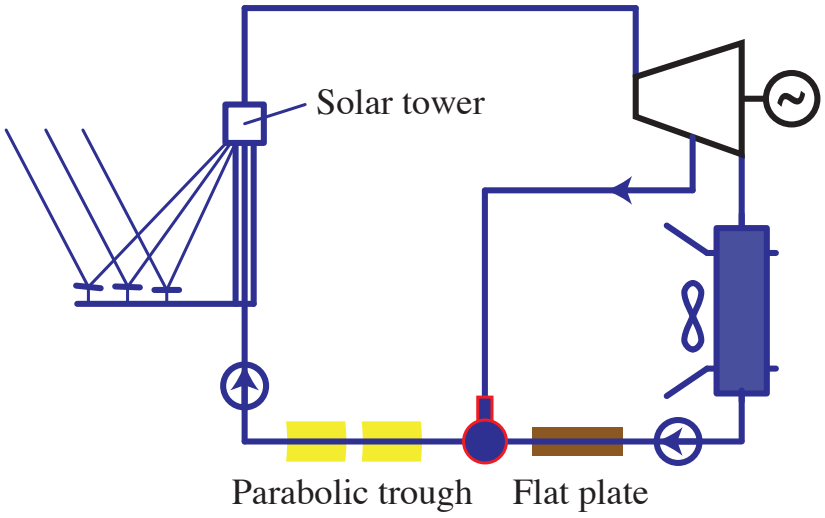

Figure 2.20: Schematic diagram of a cascade system using collector series connection

A collector series connection is proposed in section

2.2.4 Direct steam generation

Direct steam generation for solar thermal power generation has the advantage of having fewer components and no loss of temperature required with an intermediate transfer. Besides, it is clear that water is characterized by lower environmental risk than thermal oil so that leakages in a DSG power plant do not represent an environmental hazard [**?**]. Water has a lower freezing temperature than thermal oil and above all than solar salt: the efforts required to ensure adequate anti-freezing

protection are significantly reduced. Water is also less corrosive than solar salt [**?**]. With both liquid and vapor in a receiver, however, extreme care must be taken in the design of the receiver to ensure that the radiant flux incident on that portion of the receiver containing vapor is less than the flux incident in the regions with liquid and where boiling is taking place. This is because the heat-transfer coefficient into a liquid is significantly higher than into superheated vapor. For similar values of solar flux, burnout of the receiver walls could occur in the regions where vapor exists on the other side of the receiver wall.

Many concentrating collector designs require that the receiver change attitude while the collector tracks the sun. This change of attitude increases the chances of high flux on portions of the receiver containing vapor. Two examples of solar Rankine power systems where the engine working fluid vapor is generated directly in the receiver are the Solar One Pilot Plant at Barstow, CA and the solar organic Rankine cycle module built by Ford Aerospace and Communications Corporation. Because Solar One is a central receiver system, the vertical-tube receiver remains stationary and liquid level control is relatively easy. The vertical tubes of the receiver are made of a material with a high melting point and thus can withstand high temperatures in the upper regions where vapor is being superheated. Tube burnout is avoided in the Ford Aerospace receiver design because the inner wall of the receiver is a copper shell with tubes wound around its exterior. The high thermal conductivity of the copper shell provides an averaging effect on receiver temperature, and superheat is attained without burnout of the receiver walls.

All the CSP commercial plants already built apply indirect steam generation, with the exception of the 5 MWe DSG Thai Solar One (TSE-1) plant in Thailand (Thailand, 2012) [**?**]. The reason for this universally accepted choice must be found in the difficulties related to the flow control and manufacturing of equipment to be used in the presence of a two-phase flow in the absorber tubes. The behavior of the two-phase flow inside the absorber tubes of a parabolic-trough collector forces the implementation of a complex and expensive control system and the use of fast water streams in order to avoid stratified flow.

Another problem related to the DSG is the high value of the steam pressure

inside the receiver tubes that must match the turbine inlet pressure for less than pressure losses. Indeed, handling the moveable and flexible components forming the receiver tube of the collector in case of high-pressure values was one of the main problems to be faced at the early stages of the DSG concept technology.

Apply direct steam generation may be a better choice in the cascade system, however, it is not adopted for the cascade system for its immaturity.

2.2.5 Heat exchanger between circuits

Section

For the first type, it seems not economic since the temperature of the oil is not limited by the parabolic trough collectors. The temperature of the oil is constrained by the oil properties.

2.2.6 Heat recovery between cycles

footnotefootnote # Chapter 3

System modeling

To investigate the performance of the proposed cascade systems, mechanism models of the systems were developed with EES (Engineering Equation Solver) and MATLAB. Bottom-up design method was used for the system modeling. Firstly, the mechanism models of the developed in EES to validate the theoretical relationships of the models. Secondly, the component models were developed in MATLAB by using object-oriented method. It makes full use of inheritance and polymorphism to ensure both the independence and the relevance of the components. Three circuits, air circuit, water circuit and oil circuit, were developed with some specific state parameters in some key components. Energy-based models of these key components were created on the basis of their thermodynamic behavior, heat transfer and the second law.

The following parts introduce models of some key components.

3.1 Component modeling

3.1.1 Parabolic trough collector

Parabolic trough collector consists of a reflector and a receiver. The reflector (mirror) reflects direct solar radiation and concentrates it onto a receiver tube located in the focal line of the parabola. The receiver is typically a metal absorber tube with high absorption rate coating. An outer glass tube is used outside the ab-

sorber tube to reduce thermal losses and the space between the absorber tube and the glass tube is usually drawn into a vacuum to further reduce the thermal losses.

Optical loss exists in the reflection process due to optical efficiency terms. The reflection terms can be listed as bellow [**?**]:

- Shadowing factor
- Tracking error
- Geometry error
- Clean mirror reflectance
- Dirt on mirrors
- Unaccounted errors

Another term, incident angle modifier $K(\theta)$, should be concerned when the solar irradiation is not normal to the collector aperture. It is a function of the solar incidence angle to the normal of the collector aperture (θ).

The equation was determined from trough collector testing conducted at SNL [**?**].

$$K(\theta) = \cos\theta + 0.000884\theta - 0.0000536 9\theta^2 \tag{3.1}$$

The optical losses are associated with five parameters (see fig.

- Reflectivity, ρ: only a fraction of the incident radiation is reflected towards the receiver. The fraction is determined by the reflector type and dirt condition. Reflectivity of commercial parabolic trough mirrors can be assumed to be 0.9 for washed mirrors.
- Intercept factor, γ: a fraction of the direct solar radiation reflected by the mirrors does not reach the glass cover of the absorber tube due to either microscopic imperfections of the reflectors or macroscopic shape errors in the parabolic trough concentrators (e.g., imprecision during assembly). These errors cause reflection of some rays at the wrong angle, and therefore they do not intercept the absorber tube. These losses are quantified by an optical parameter called the intercept factor, γ, that is typically 0.95 for a collector properly assembled.

- Transmissivity of the glass tube, τ: only a fraction of the direct solar radiation reaching the glass cover of the absorber pipe is able to pass through it. The ratio between the radiation passing through the glass tube and the total incident radiation on it, gives transmissivity τ, which is typically 0.93.
- Absorptivity of the absorber selective coating, α_{abs}: this parameter quantifies the amount of energy absorbed by the steel absorber pipe, compared with the total radiation reaching the outer wall of the steel pipe. This parameter is typically 0.95 for receiver pipes with a cermet coating, whereas it is slightly lower for pipes coated with black nickel or chrome.
- Soiling factor, F_e: because of the dirt on reflectors will reduce the reflectivity, it needs to concern the soiling factor. The soiling factor F_e takes into account the progressive soiling of mirrors and glass tubes after washing.

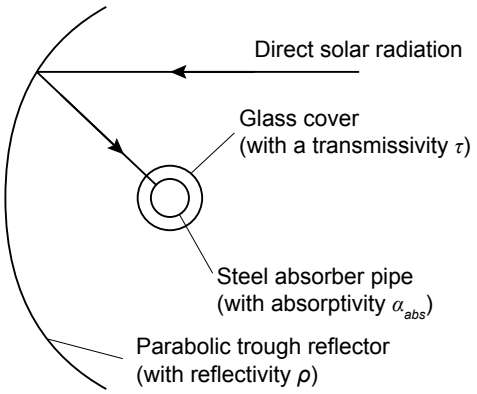

Figure 3.1: Some of the optical parameters of a parabolic trough

The energy pass through the glass tube to the receiver can be obtained by

$$P = I_r w_{tc} L_{tc} \rho \gamma \tau F_e K(\theta) \tag{3.2}$$

The solar energy absorbed by the absorber occurs very close to the outer surface, to simplify the absorption process, it is treated as a uniform heat flux q''. q''Heat flux

$$q'' = \frac{P}{\pi d_o L_{tc}} = \frac{I_r w_{tc} \rho \gamma \tau F_e K(\theta)}{\pi d_o} \tag{3.3}$$

Assume overall heat transfer coefficient $U(T_{abs})$ is uniform for whole length of the collector, and the heat transfer correlation in Appendix **??** can be used. Figure

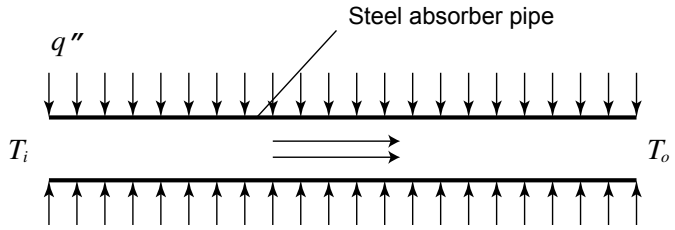

Figure 3.2: Schematic diagram of the absorber pipe

Since the Nusselt number Nu in the pipe is very large (about 1×10^4), small temperature difference exists between the absorber and oil. So the average fluid temperature $(T_i + T_o)/2$ can be used as the average value of T_{abs}, and $U(T_{abs})$ can be obtained by the a second-order polynomial function given by Romero [**?**]. The length L required to get the required number of trough collectors in a row can be obtained from Equation (

3.1.2 Parabolic dish collector

Parabolic dish collector consists of a reflector and a receiver. The reflector (mirror) tracks the sun to reflect direct solar radiation and concentrates it onto a receiver located at the focal point of the reflector. Two axes tracking system needs to be applied for the reflector to continuously follow the daily path of the sun.

In a traditional dish-Stirling system, a Stirling engine is located at the focal point. The Stirling engine has a receiver to absorb the thermal energy from the concentrated sunlights. The receiver consists of an aperture and an absorber. The aperture in a Stirling receiver is located at the focal point of the reflector to reduce the radiation and convection losses. The absorber absorbs the solar radiation and transfers the thermal energy to the working gas of the Stirling engine. An electrical generator, directly connected to the crankshaft of the engine, converts the mechanical energy into electricity.

In the proposed cascade system, a volumetric receiver is located on the focal point. Spiral tube is located in the receiver to absorb the concentrated solar energy. Air (or nitrogen, is used as the heat transfer fluid) flows trough the tube to transfer the absorbed energy as the heat source of Stirling engine(s).

The reflector is a key element of the systems. The curved reflective surface can be manufactured by attached segments, by individual facets or by a stretched membranes shaped by a continuous plenum. In all cases, the curved surface should be coated or covered by aluminum or silver reflectors.

Two different methods [**?**] are applied for the sun tracking systems:

- Azimuth elevation tracking by an orientation sensor or by calculated coordinates of the sun performed by the local control.
- Polar tracking, where the concentrator rotates about an axis parallel to the earth's axis rotation.

A dish reflector product of SES (Stirling Energy System) is used in this cascade system, and its key parameters can be found in Table

Table 3.1: Key parameters of the dish collector

Parameter	Value	Parameter	Value	Parameter	Value
d_{cav}	$0.46\,\mathrm{m}$	ϵ_{insu}	0.6	θ_{dc}	45°
δ_{insu}	$0.075\,\mathrm{m}$	α_{cav}	0.87	γ	0.97
dep_{cav}	$0.23\,\mathrm{m}$	δ_a	$0.005\,\mathrm{m}$	$\eta_{shading}$	0.95
d_{ap}	$0.184\,\mathrm{m}$	$d_{i,1}$	$0.07\,\mathrm{m}$	ρ	0.91
λ_{insu}	$0.06\,\mathrm{W/(m\cdot K)}$	A_{dc}	$87.7\,\mathrm{m}^2$		

[G]δThickness, m [S]$insu$insulating layer depDepth, m dDiameter, m [G]λThermal conductivity, $\mathrm{W/(m\cdot K)}$ [G]ϵEmissivity [G]θ_{dc}Dish aperture angle (0° is horizontal, 90° is vertically down) [G]γIntercept factor; compression ratio [G]$\eta_{shading}$Shading factor [G]ρReflectivity $A_{se,1}$Heat transfer area of Stirling engine at air side, m^2 $A_{se,2}$Heat transfer area of Stirling engine at water side, m^2 kSpecific heat ratio

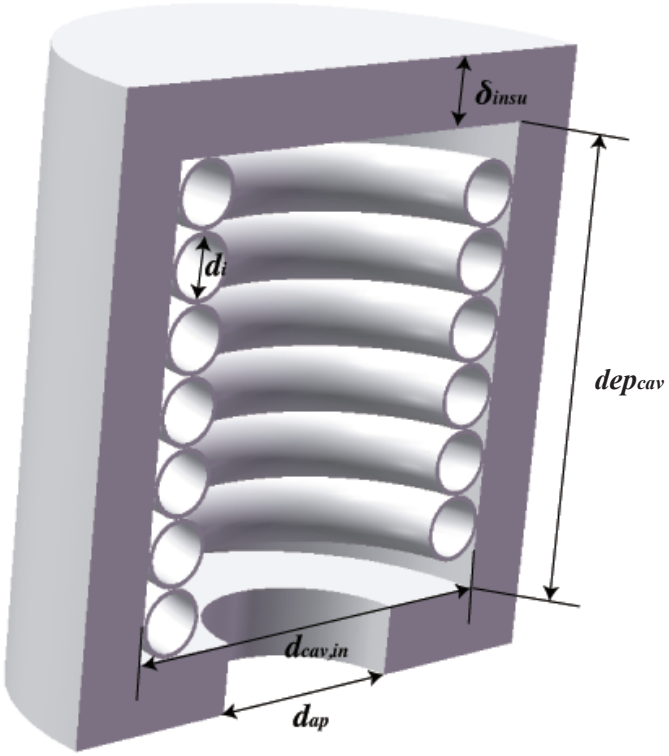

Figure 3.3: The structure of the dish receiver

n_gAmount of working gas in each Stirling engine, mol n_{se}Number of Stirling engines in the Stirling engine array

The dish receiver model concerns the losses include: collector losses due to mirror reflectivity, receiver intercept losses, losses due to shading, and thermal losses. Thermal losses take the largest portion of all those losses, which are due to conduction, convection and radiation. Figure

To solve the thermal network in fig.

1. *Inlet energy from the reflector,* q_i

   To simplify the model, influences made by receiver blocking and imperfection track are ignored.

$$q_i = I_r A_{dc} \gamma \eta_{shading} \rho \tag{3.4}$$

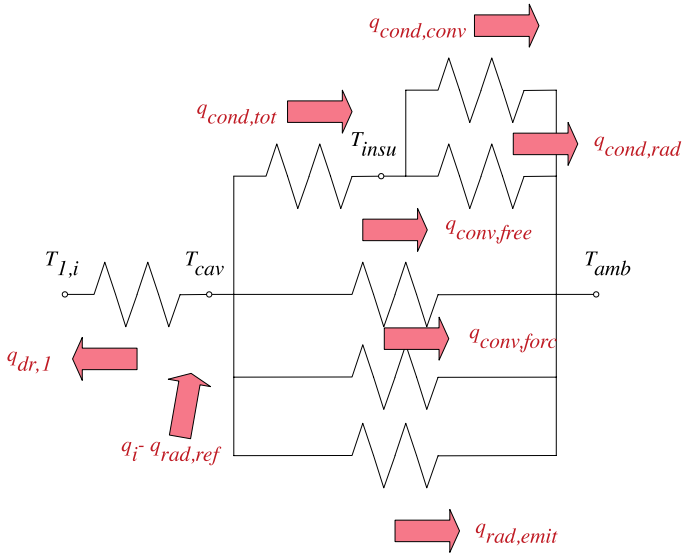

Figure 3.4: Thermal network of dish receiver

In equation

The heat transfer process between the HTF and the dish absorber is simplified to a heat exchange process of a flow in a uniform temperature heat pipe. So $q_{dr,1}$ can be written as

$$q_{dr,1} = h_{dr,1} A_{dr,1} \Delta T_{ln,dr,1} \tag{3.5}$$

$A_{dr,1}$Heat transfer area of dish receiver between tube and air, m^2 where

$$h_{dr,1} = Nu_{tube} \lambda_{dr,1} / d_{i,1} \tag{3.6}$$

$$Nu_{tube} = c_r Nu'_{tube} \tag{3.7}$$

NuNusselt number c_rHeat transfer correction factor of coiled tube of volumetric receiver For helical spiral pipe, multiplier c_r based on curvature ratio can be written as [**?**]

$$c_r = 1 + 3.5 \frac{d_{i,1}}{d_{cav} - d_{i,1} - 2\delta_a} \tag{3.8}$$

Nu'_{tube} is the Nusselt number of straight circular tube, which can be obtained by [**?**]

$$Nu'_{tube} = 0.027 Re_{tube}^{0.8} Pr_{tube}^{1/3} (\mu_{tube}/\mu_{tube,w})^{0.14} \tag{3.9}$$

PrPrandtl number ReReynolds number [G]μViscosity, kg/(m·s) [S]wTube wall and the logarithmic mean temperature difference $\Delta T_{ln,dr,1}$ can be written as

$$\Delta T_{ln,dr,1} = \frac{(T_{cav} - T_{dc,i}) - (T_{cav} - T_{dc,o})}{\ln \dfrac{T_{cav} - T_{dc,i}}{T_{cav} - T_{dc,o}}} \tag{3.10}$$

2. *Radiation losses reflected off the receiver,* $q_{rad,ref}$

$$q_{rad,ref} = (1 - \alpha_{eff}) q_i \tag{3.11}$$

where α_{eff} is the effective absorptivity of the receiver.

$$\alpha_{eff} = \frac{\alpha_{cav}}{\alpha_{cav} + (1 - \alpha_{cav}) \dfrac{A_{ap}}{A_{cav}}} \tag{3.12}$$

α_{cav} is the absorptivity of the cavity, A_{cav} is the cavity area, A_{ap} is the aperture area.

3. *Conductive losses through the receiver insulating layer,* $q_{cond,tot}$

$$q_{cond,tot} = 2\pi \lambda_{insu} dep_{cav} \frac{T_{cav} - T_{insu}}{\ln((d_{cav} + 2\delta_{insu})/d_{cav})} \tag{3.13}$$

where T_{cav} is the temperature of the cavity wall, T_{insu} is outside temperature of the insulation wall.

4. *Convection losses from the receiver insulating layer,* $q_{cond,conv}$

$$q_{cond,conv} = h_{insu} A_{insu} (T_{insu} - T_{amb}) = \frac{k_{insu} Nu_{insu} A_{insu} (T_{insu} - T_{amb})}{d_{cav} + 2\delta_{insu}} \tag{3.14}$$

k_{insu}Thermal conductivity of air at the temperature of outside insulating layer, W/(m·K) where Nu_{insu} can be obtained by the correlation for flow over a circular cylinder. [**?**]

5. *Radiation losses from the receiver insulating layer,* $q_{cond,rad}$

$$q_{cond,rad} = \epsilon_{insu} A_{insu} \sigma (T_{insu}^4 - T_{amb}^4) \tag{3.15}$$

6. *Free convection from the cavity in the absence of wind,* $q_{conv,free}$

   Ma [**?**] conducted tests to determine the free convection losses from the receiver for alternative setups, and the data were consistent with Stine and McDonald's free convection correlation. It is assumed that forced convection is independent of free convection in the receiver, so the total convection losses can be represented as the total of the free and forced convection losses as shown in Figure

7. *Force convection from the cavity in the presence of wind,* $q_{conv,forc}$

$$q_{conv,forc} = h_{forc} A_{cav} (T_{cav} - T_{amb}) \tag{3.16}$$

   Wu [**?**] present a comprehensive review and systematic summarization of convection heat loss from cavity receiver in parabolic dish solar thermal power system. And we choose the correlation presented by Leibfried [**?**]. This correlation gives an extended model of Koenig [**?**] and Stine [**?**] with better results.

   For forced convection loss, side-on wind convection loss model given by Ma [**?**], which is independent of the aperture orientation, is used

$$h_{forc} = 0.1967 v_{wind}^{1.849} \tag{3.17}$$

8. *Emission losses due to thermal radiation emitted from the receiver aperture,* $q_{rad,emit}$

   The emissivity is set equal to the effective absorptivity of the cavity (gray body),

$$\epsilon_{cav} = \alpha_{eff} \tag{3.18}$$

$$q_{rad,emit} = \epsilon_{cav} A_{ap} \sigma (T_{cav}^4 - T_{amb}^4) \tag{3.19}$$

From fig

$$q_{dr,1} = q_i - q_{rad,ref} \tag{3.20}$$

$$q_{dr,1} = q_{cond,tot} + q_{conv,free} + q_{conv,forc} + q_{rad,emit} \tag{3.21}$$

$$q_{cond,tot} = q_{cond,conv} + q_{cond,rad} \tag{3.22}$$

So the temperature nodes in the thermal network can be solved by these equations.

$q_{dr,1}$ can be obtained by Equation

3.1.3 Stirling engine

3.1.3.1 Theoretical Stirling cycle

In a Stirling cycle, there are two isothermal processes that exchange heat with heating and cooling fluids, two isochoric processes that exchange heat with regenerator. In Figure

In order to obtain a simplified analytical model, several simplifications were made:

- The working gas in Stirling engines obeys the idea gas law.
- No heat loss to the environment for Stirling engines.
- Overall heat transfer coefficients of the fluids are constant.
- A symmetrical regenerator behavior is assumed [**?**, **?**] so that a simple effectiveness can be obtain by $T_R = \frac{T_H - T_L}{\ln(T_H/T_L)}$.

To consider internal irreversibilities in Stirling cycle made by dead volumes, as described in Duan's paper [**?**], total dead volume V_D is divided into heater dead volume V_{DH}, regenerator dead volume V_{DR} and cooler dead volume V_{DC}. There

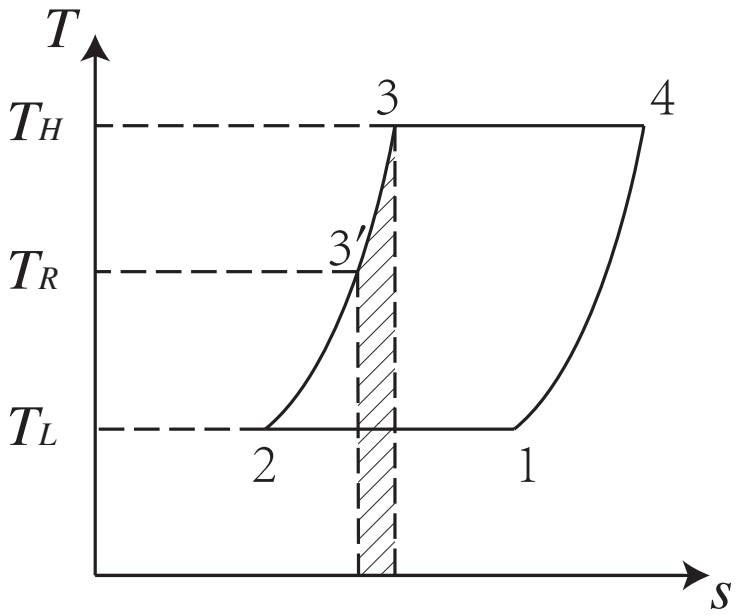

Figure 3.5: T-s diagram of a Stirling cycle

exists a factor K to describe the dead volumes under different temperatures. K is relevant with temperatures in the process and regenerator effectiveness. $V_D$total dead volume (m^3) V_{DH}hot space dead volume (m^3) V_{DR}regenerator dead volume (m^3) V_{DC}cold space dead volume (m^3)

$$K = \frac{V_{DH}}{T_H} + \frac{V_{DR}}{T_R} + \frac{V_{DC}}{T_L} \tag{3.23}$$

Kdead volume factor

For the isothermal compression process 1-2, the output work

$$W_{12} = \int_{V_E+V_C}^{V_E} p_{12} dV = -mRT_L \ln \frac{V_E + V_C + KT_L}{V_E + KT_L} \tag{3.24}$$

$V_E$expansion volume (m^3) $V_C$compression volume (m^3) $m$mass of working fluid in Stirling engine (kg) Rgas constant (J·kg^{-1}·K^{-1})

For the isothermal expansion process 3-4, the output work

$$W_{34} = \int_{V_E}^{V_E+V_C} p_{34} dV = mRT_H \ln \frac{V_E + V_C + KT_H}{V_E + KT_H} \tag{3.25}$$

Define $\gamma_H = \frac{V_E+V_C+KT_H}{V_E+KT_H}$, and $\gamma_L = \frac{V_E+V_C+KT_L}{V_E+KT_L}$, so in a cycle, the theoretical output work [G]$\gamma_H$space ratio in process 12 [G]$\gamma_L$space ratio in process 34

$$W_{th} = W_{12} + W_{34} = mR(T_H \ln \gamma_H - T_L \ln \gamma_L) \tag{3.26}$$

Woutput work (J) [S]ththeoretical

For the isochoric heating process 3'-3, the absorbed heat

$$Q_{3'3} = nc_v(T_H - T_R) = \frac{1-e}{k-1} mR(T_H - T_L) \tag{3.28}$$

$c_v$specific heat at constant volume (J·kg^{-1}·K^{-1}) $k$specific heat ratio (c_p/c_v), thermal conductivity (W $\cdot$ m^{-1} $\cdot$ K^{-1})

For the the isothermal expansion process 3-4, the absorbed heat

$$Q_{34} = W_{34} = mRT_H \ln \gamma_H \tag{3.29}$$

In a cycle, the theoretical absorbed heat

$$Q_{th} = Q_{3'3} + Q_{34} = \frac{1-e}{k-1} mR(T_H - T_L) + mRT_H \ln \gamma_H \tag{3.30}$$

Qabsorbed heat (J)

Ppower of Stirling engine (W) s_{se}speed of Stirling engine (Hz)

3.1.3.2 Irrevisibilities and losses

1. Non-ideal heat transfer effect

   Because of non-ideal heater and cooler, the working fluid temperature (T_H/T_L) in these two heat exchangers is less/higher than the wall temperature (T_{hw}/T_{cw}), respectively. And T_H and T_L can be corrected by the wall temperatures as follows:

   $$T_H = T_{hw} - \frac{Qs_{se}}{h_h A_{hw}} \tag{3.31}$$

   [S]hwheater wall

   $$T_L = T_{cw} + \frac{(Q-W)s_{se}}{h_c A_{cw}} \tag{3.32}$$

   [S]cwcooler wall

The heat transfer coefficient can be obtained using the following correlation [**?**]:

$$h_{h,c} = \frac{\mu c_p f_{Re}}{2 D_{h,c} Pr_{h,c}} \tag{3.33}$$

[G]μdynamic viscosity (kg $\cdot$ m^{-1} $\cdot$ s^{-1})

where f_{Re} is a Reynolds friction factor defined as:

$$f_{Re} = 0.0791 {Re_{h,c}}^{0.75} \tag{3.34}$$

$Re_{h,c}$, $Pr_{h,c}$ and $D_{h,c}$ are Reynolds number, Prandtl number and hydraulic diameter of the heater/cooler exchanger.

2. Effect of pressure drop

   Pressure drops in the heat exchangers cause power losses of the Stirling engine. The pressure drops can be obtained by [**?**]:

$$\Delta p = -\frac{2 f_{Re} \mu u V}{d^2 A} \tag{3.35}$$

   $p$pressure (Pa)

   where u is the working gas speed, V is volume, A is flow cross-section area.

   The net power loss of the Stirling engine due to pressure drop of the heat exchangers can be evaluated by:

$$W_{pd} = \oint \sum_{i=E,C} (\Delta p_i \frac{dV_i}{d\theta}) d\theta \tag{3.36}$$

3. Effect of finite speed of piston and mechanical friction

   Due to the finite speed of piston, the pressure on the piston surface is different from the pressure of expansion and compression spaces. It has been demonstrated that the pressure on the piston surface in the expansion process is less than the mean pressure in the expansion space. Similarly, the pressure on the piston surface in the compression process is greater than the mean pressure in the compression space. This means the output work is less than the theoretical value. Besides, The output work also reduces due to mechanical

friction. The output work loss due to finite speed of piston and mechanical friction can be obtained as follows [**?**]:

$$W_{fs} = \oint p(\pm\frac{au_p}{c} \pm \frac{\Delta p_f}{p})dV \tag{3.37}$$

where the sign (+) is used in the compression space, and the sign (-) is used in the expansion space. p is the mean pressure in the compression/expansion space, u_p is velocity of the piston, c is the average speed of molecules and Δp_f is the pressure loss due to mechanical friction. Δp_f, a and c can be obtained by [**?**]:

$$\Delta p_f = 0.97 + 0.009 s_{se} \tag{3.38}$$

$$a = \sqrt{3k} \tag{3.39}$$

$$c = \sqrt{3RT} \tag{3.40}$$

4. Energy losses due to internal conduction

   The temperature differs from the heater and cooler, heat losses from heater to cooler exists due to internal conduction through the walls of regenerator. [**?**] The internal conduction loss in a cycle can be obtained by follows:

$$Q_{id} = \frac{k_r A_r}{L_r s_{se}}(T_{hw} - T_{cw}) \tag{3.41}$$

   where, k_r, A_r and L_r denote the regenerator matrix conductivity, regenerator length, and regenerator conductive area respectively. [S]$r$regenerator

5. Energy losses due to shuttle conduction

   The displacer shuttles between the expansion and compression space. It absorbs heat during the hot end of its stroke and releases it during the cold end of its stroke. This heat loss can be estimated as [**?**]:

$$Q_{sc} = 0.4\frac{Z^2 k_p D_p}{J L_d s_{se}}(T_H - T_L) \tag{3.42}$$

   where, Z, k_p, D_p, J and L_d denote the displacer stroke, piston thermal conductivity, displacer diameter, gap between the displacer and the cylinder,